HHS Public Access

Author manuscript

Brain Res Bull. Author manuscript; available in PMC 2019 March 01.

Published in final edited form as:

Brain Res Bull. 2018 March ; 137: 53–70. doi:10.1016/j.brainresbull.2017.11.007.

CaMKIIα expression in a mouse model of NMDAR hypofunction schizophrenia: putative roles for IGF-1R and TLR4

OM Ogundele[1] and **CC Lee**[1]

[1]Department of Comparative Biomedical Sciences, Louisiana State University School of Veterinary Medicine, Baton Rouge, Louisiana

Abstract

Schizophrenia (SCZ) is a neuropsychiatric disorder that is linked to social behavioral deficits and other negative symptoms associated with hippocampal synaptic dysfunction. Synaptic mechanism of schizophrenia is characterized by loss of hippocampal N-Methyl-D-Aspartate Receptor (NMDAR) activity (NMDAR hypofunction) and dendritic spines. Previous studies show that genetic deletion of hippocampal synaptic regulatory calcium-calmodulin dependent kinase II alpha (CaMKIIα) cause synaptic and behavioral defects associated with schizophrenia in mice. Although CaMKIIα is involved in modulation of NMDAR activity, it is equally linked to inflammatory and neurotropin signaling in neurons. Based on these propositions, we speculate that non-neurotransmitter upstream receptors associated with neurotropic and inflammatory signaling activities of CaMKIIα may alter its synaptic function. Besides, how these receptors (i.e. inflammatory and neurotropic receptors) alter CaMKIIα function (phosphorylation) relative to hippocampal NMDAR activity in schizophrenia is poorly understood. Here, we examined the relationship between toll-like receptor (TLR4; inflammatory), insulin-like growth factor receptor 1 (IGF-1R; neurotropic) and CaMKIIα expression in the hippocampus of behaviorally deficient schizophrenic mice after we induced schizophrenia through NMDAR inhibition.

Schizophrenia was induced in WT (C57BL/6) mice through intraperitoneal administration of 30mg/Kg ketamine (NMDAR antagonist) for 5 days (WT/SCZ). Five days after the last ketamine treatment, wild type schizophrenic mice show deficiencies in sociability and social novelty behavior. Furthermore, there was a significant decrease in hippocampal CaMKIIα ($p<0.001$) and IGF-1R ($p<0.001$) expression when assessed through immunoblotting and confocal immunofluorescence microscopy. Additionally, WT schizophrenic mice show an increased percentage of phosphorylated CaMKIIα in addition to upregulated TLR4 signaling (TLR4, NF-κB, and MAPK/ErK) in the hippocampus. To ascertain the functional link between TLR4, IGF-1R and CaMKIIα relative to NMDAR hypofunction in schizophrenia, we created hippocampal-specific TLR4 knockdown mouse using AAV-driven Cre-lox technique (TLR4 KD). Subsequently, we inhibited NMDAR function in TLR4 KD mice in an attempt to induce schizophrenia (TLR4

Co-Corresponding Authors: Olalekan M. Ogundele (ogundele@lsu.edu). Charles C. Lee (cclee@lsu.edu).

Competing interests: The author states that the present manuscript presents no conflict of interest.

KD SCZ). Interestingly, IGF-1R and CaMKIIα expressions were preserved in the TLR4 KD hippocampus after attenuation of NMDAR function. Furthermore, TLR4 KD SCZ mice showed no prominent defects in sociability and social novelty behavior when compared with the control (WT).

Our results show that a sustained IGF-1R expression may preserve the synaptic activity of CaMKIIα while TLR4 signaling ablates hippocampal CaMKIIα expression in NMDAR hypofunction schizophrenia. Together, we infer that IGF-1R depletion and increased TLR4 signaling are non-neurotransmitter pro-schizophrenic cues that can reduce synaptic CaMKIIα activity in a pharmacologic mouse model of schizophrenia.

Keywords

Schizophrenia; NMDAR; IGF-1R; CaMKIIα; MAPK/ErK; TLR4

Introduction

Schizophrenia affects approximately 1.1% (~83 Million people) of the world's population across all sex, age and background (NIH-NIMH, 2017; SARDAA, 2017). About 3.5 Million people are affected in the United States and it is one of the leading causes of disability (NIH-NIMH, 2017; SARDAA, 2017). While the disorder is partially genetic, stress and drugs are predominant causes of schizophrenia. Importantly, 75% of individuals that become schizophrenic show the symptoms in late adolescence to early adulthood (age 16–25yrs) (NIH-NIMH, 2017; SARDAA, 2017; Arian et al., 2013). This coincides with the peak of brain wiring, then re-wiring (age 22–25yrs) required for transitioning from childhood to adult brain (Arian et al., 2013; Owens et al., 2012; Owen and O'Donovan, 2012; Eckfeld et al., 2017). In schizophrenia, this generally involves changes in expression of neurotransmitters (glutamate and dopamine), receptors (**NMDAR;** N-Methyl-D-Aspartate receptor and **D_2R;** Dopaminergic D_2 receptor), and proteins involved in the regulation of their synaptic activities (Nazakawa et al., 2017; Cohen et al., 2015; Dias, 2012; Barkus et al., 2012; Seillier and Giuffrida, 2009). As such, most available treatment methods involve the use of antipsychotics that target these receptors (i.e. NMDAR and D_2R). Side effects of these drugs are a limitation as it often leads to depression, movement disorders and catalepsy (Amodeo et al., 2017; Nakata et al., 2017, Nikvarz et al., 2017; Freyberg et al., 2017; Ibi et al., 2017; Meltzer, 2017; Ostinelli et al., 2017; Su et al., 2017). Therefore, there is a need for assessment of other synaptic targets that can reduce synaptic and behavioral defects of schizophrenia while circumventing neurotransmitter receptor sensitivity (Yang and Tsai, 2017).

Despite the limitations, treatment methods that target dopamine and glutamate receptors are laudable based on vastly studied dopamine and glutamate hypothesis of schizophrenia (Yang and Tsai, 2017; Purves-Tyson et al., 2017; Howes et al., 2017). However, the significance of synaptic regulatory calcium-calmodulin-depended kinase 2 alpha (CaMKIIα) – linked with synaptic function of NMDAR (Hahgihara et al., 2014; Hagihara et al., 2013; Purkayastha et al., 2012; Dhavan et al., 2002; Robison et al., 2005) and D_2R (Ng et al., 2010; Takeuchi et al., 2002; Vekshina et al., 2017) - cannot be over emphasized in schizophrenia. Substantive

evidence now exists to confirm that genetic deletion of CaMKIIα is a cause of synaptic and behavioral changes that are characteristic of schizophrenia (Frankland et al., 2008; Matsuo et al., 2009; Yamasaki et al., 2008). Roles of CaMKIIα in neurons are wide and varied. CaMKIIα is involved in inflammatory signaling that is linked with toll-like receptor 4 (TLR4/NF-κB) (Kaltschmidt et al., 2005; Mémet, 2006). Additionally, it acts downstream of IGF-1R-Ras/Raf pathway to regulate calcium-mediated synaptic activity of NMDAR (Hu et al., 2016; Le Grevès et al., 2005; Dou et al., 2005). Based on these propositions, it is logical to speculate that synaptic and inflammatory activity of CaMKIIα are not mutually exclusive. Although CaMKIIα depletion has been implicated in schizophrenia (Matsuo et al., 2009; Yamasaki et al., 2008), the mechanism through which IGF-1R and TLR4 can putatively affect synaptic CaMKIIα expression in pathophysiology of schizophrenia is poorly understood.

Localization of CaMKIIα at post-synaptic sites enables interactions with neurotrophic factors and receptors involved in synaptic development and maintenance (Hami et al., 2014; Kiray et al., 2014; Sun, 2006; Gunnell et al., 2007; Venkatasubramanian et al., 2010; Demirel et al., 2014). Moreover, loss of these proteins have been implicated in several developmental neuropsychiatric disorders including schizophrenia (Nelson et al., 2006; Ribasés et al., 2008). Among these, IGF-1R may alter CaMKIIα expression through Wnt/GSK3 and Ras/Raf signaling in growth, synaptic function, inflammation, and cell death (Pereira et al., 2008). Furthermore, both IGF-1R and CaMKIIα promotes pre- and post-synaptic calcium movement linked to NMDAR function in the hippocampus during long-term potentiation (LTP) and cognition (Cassilhas et al, 2012; Hu et al., 2016). In addition to the control of growth and aging, a recent study demonstrates the significance of IGF-1R signaling in presynaptic calcium release and glutamatergic neurotransmission. In their study, Gazit and co-workers show that IGF-1R modulates calcium release from the mitochondria and regulate presynaptic activity of synaptophysin (Gazit et al., 2016). Equally, IGF-1R signaling alters protein kinase systems (Akt/mTOR and MAPK/ErK) (Dyer et al., 2016; Netchine et al., 2011; Salani et al., 2015) involved in the regulation of neurodevelopment and LTP (Zheng et al., 2012; Kéri et al., 2011; Romanelli et al., 2007). Owing to its effect on synaptic calcium currents (Gazit et al., 2016) and gene expression (Le Grevès et al., 2005; Le Grevès et al., 2006), IGF-1R may significantly affect the activity of ionotropic glutamate receptors in normal LTP and disease conditions (Jiang et al., 2015; Demirel et al., 2014; Gunnell et al., 2007).

The function of CaMKIIα is not restricted to neurotropic regulation of growth, and synaptic function. Downstream of IGF-1R, CaMKIIα can reduce the activity of proinflammatory proteins like NF-κB and MAPK/ErK, and purigenic receptors such as TLR4 and $P2RX_7$ (Meffert and Baltimore, 2005; Luo et al., 2008; Gómez-Villafuertes et al., 2015; Huang et al., 2009). Therefore, a reduction of CaMKIIα activity can lead to inflammation and progression of synaptic dysfunction associated with schizophrenia. Evidently, the expression of TLR4 and associated pro-inflammatory proteins increases in the blood of clinically-diagnosed schizophrenia patients (Venkatasubramanian and Debnath, 2013; Chang et al., 2011; Hansen et al., 2008; McQuillin et al., 2009). In addition to their involvement in inflammation, proteins like NF-κB and MAPK/ErK – in the TLR4 signaling pathway – are known to reduce synaptic activity of CaMKIIα by increasing CaMKIIα phosphorylation

(Meffert and Baltimore, 2005; Han et al., 2009). Furthermore, MAPK/ErK and CaMKIIα occupy similar sites at post-synaptic densities where MAPK/ErK phosphorylates CaMKIIα during early and late LTP phases (Du et al., 2004; Giovanni et al., 2001; Tsui et al., 2005; Derkach et al., 2007). Although primarily inflammatory, TLR4 is involved in synaptogenesis as it increases glutamatergic function in the developing brain (Shen et al., 2016; Henneberger and Steinhäuser, 2016). This is required for the development and formation of synapses by migrating neurons (Shen et al., 2016; Venkatasubramanian and Debnath, 2013). However, in excess, TLR4-linked glutamate release may induce epileptogenic effects and other forms of excitotoxicity through an upregulated MAPK/ErK signaling (Jiang et al., 2015; Shen et al., 2016; Henneberger and Steinhäuser, 2016). Since MAPK/ErK also act downstream of IGF-1R (Xing et al., 2016; Dyer et al., 2016; Vahdatpour et al., 2016), neural activity of TLR4 may overlap with neurotropic cues of IGF-1R and other kinase receptors involved in nervous system development and neural circuit formation (Fig. 1). Thus, an increased TLR4 signaling may upregulate MAPK/ErK which can abolish IGF-1R signaling and CaMKIIα activities in the brain.

Based on these propositions, we hypothesize that NMDAR-linked CaMKIIα activity in synaptic function and neurotropic signaling are not exclusive of its fate in inflammation. In brief, CaMKIIα modulates synaptic NMDAR function (Mao et al., 2014; Ma et al., 2015; Park et al., 2008; Johnston and Morris, 1995), and itself (i.e CaMKIIα) can be altered through TLR4 and IGF-1R signaling. Through upregulated MAPK/ErK, TLR4 may alter synaptic function by reducing IGF-1R signaling. This may lead to a reduced CaMKIIα activation downstream of IGF-1R (Ras/Raf), and increased CaMKIIα phosphorylation (inactivation) by MAPK/ErK. Therefore, decreased TLR4 and upregulated IGF-1R signaling are possible mechanisms through which CaMKIIα activity can be preserved in NMDAR hypofunction. Here, we show that induced loss of NMDAR function can cause hippocampal CaMKIIα loss and decrease IGF-1R signaling. Furthermore, we tested the effectiveness of hippocampal-specific TLR4 knockdown as an intervention method to preserve IGF-1R and CaMKIIα in mice after a persistent NMDAR inhibition.

Materials and Methods

Animal Strains

Adult C57BL/6 (WT) and transgenic C57BL/TLR4$^{loxp/loxp}$ (TLR4 floxed mice) weighing between 22–25 grams were used for this study. All Animals were procured from Jackson Lab and housed in the LSU School of Veterinary Medicine vivarium. Mice were handled in accordance with the Institutional Animal Care and Use Committee at the Louisiana State University.

Adeno-associated viral Gene Expression

AAV-CMV-eGFP and AAV-CMV-Cre-eGFP were procured from the University of Iowa Vector Core (Iowa City, IA) and stored at −80°C. Transgenic TLR4$^{loxp/loxp}$ (floxed) mice were anaesthetized using Ketamine/Xylazine (i.p. 100mg/Kg:10mg/Kg). For n=30 TLR4 floxed mice, AAV cocktail (AAV-CMV-eGFP; n=15 mice and AAV-CMV-Cre-eGFP; n=15 mice) was stereotactically injected into the hippocampus (DG/CA1 field) at coordinates [AP

−1.93, ML+2.3mm, DV+2.5mm] relative to the bregma (Franklin and Paxinos, 1997). AAV cocktails (500nL) were injected using a low-resistance flame-pulled glass pipette (200μm tip) filled with mineral oil and mounted on a Nanoject (Drummond Instruments, USA). AAV cocktail was drawn into the tip of the pipette and tested for flow before being lowered into the neural tissue at the previously described coordinates. The injections were done in multiple boli (4.6 nL each) at 30 secs interval. After the last injection, the pipette stayed in position for 120 secs before it was gradually withdrawn. Animals were maintained for a 3-week survival period to allow for adequate gene expression. The set of TLR4 floxed mice expressing *Cre* in the hippocampus were designated TLR4 knockdown (TLR4 KD) while mice expressing control AAV were designated TLR4 floxed.

NMDAR Hypofunction SCZ Model

We employed the method previously described by Becker et al. (2003). Briefly, schizophrenia was induced in mice by administering (intraperitoneal) a sub-chronic dose of the non-selective NMDAR antagonist ketamine (30mg/Kg body weight) for five consecutive days (n=20 mice). After the last treatment, the animals were maintained for 4–5 days before being assessed for social interaction behavioral deficits.

Experimental groups

Firstly, we investigated the effect of induced NMDAR hypofunction on neural expression of IGF-1R, TLR4 and CaMKIIα in wild type mice. Therefore, a WT (Control) group was compared with WT mice for which we induced NMDAR hypofunction (WT/SCZ). Subsequently, we created transgenic hippocampal-specific TLR4 knockdown model to test whether attenuation of TLR4 can rescue IGF-1R and CaMKIIα loss after an induced NMDAR hypofunction. For this purpose, we created TLR4 KD SCZ and TLR4 floxed SCZ groups. However, in the analysis, WT, WT/SCZ, TLR4 floxed SCZ and TLR4 KD SCZ groups were compared.

Sociability and social novelty tests

Social interaction was assessed using the method previously described by Kaidanovich-Beilin et al. (2011). Mice were habituated in the testing area for 24 hours before the commencement of behavioral test (WT: n=15, WT/SCZ: n=20; TLR4 floxed SCZ: n=12 and TLR4 KD SCZ: n=15). Two smaller holding compartments in the testing area were designated “E (Empty)” in subsequent habituation phase (5 minutes). At each phase of the test, chamber compartments were wiped clean with 70% isopropyl alcohol to prevent odor specific cues and bias in subsequent behavioral test steps. For the sociability test, a strange mouse ($S1_a$-stranger 1) was introduced into one compartment while the other compartment remained empty (E). Subsequently, a subject mouse was placed in the test chamber for 5 minutes. After an inter-trial time of 30 minutes, chambers were again wiped clean with isopropyl alcohol following which a second strange mouse (S2) was introduced along with the first strange mouse (now $S1_b$) into two holding compartments of the sociability chamber (Fig. 2a). Contact time (secs) with E versus $S1_a$, and $S1_b$ versus S2 were estimated to determine sociability [$S1_a/(E+S1_a)$] and social novelty [$S2/(S2+S1_b)$] respectively. While “a” represents the first encounter with S1 during sociability test, “b” represents a second encounter with S1 during the social novelty test. Therefore, different time measurements

were done at $S1_a$ and $S1_b$. However, the same animal was used at both stages (Fig. 2a). Time spent in contact with E, S2, $S1_a$ and $S1_b$ during sociability and social novelty tests were estimated blindly by three investigators using Any-Maze software (Version 5.1; Stoelting Co., Wood Dale, IL).

Silver impregnation

Using Golgi-Cox staining, we examined the morphology of hippocampal dendritic spines in control and behaviorally characterized experimental schizophrenic mice and control (WT: n=10, WT/SCZ: n=10; TLR4 floxed SCZ: n=7 and TLR4 KD SCZ: n=8). Unfixed sections were processed using FD Neurotech Golgi staining kit (#PK401A) in accordance with manufacturer's instruction. Subsequent counter staining was done in cresyl fast violet (FD Neurotech; PS102-01) and mounted using histomount medium (National Diagnostics; HS-103). Images were acquired using a Nanozoomer microscope (Hamatsu, USA). Dendritic spine count was done manually for n=12 consecutive section (serial) per mice. We considered spine count/μm^2 for n=40 neurons – in CA1/DG field - per animal.

Electron Microscopy

Brain sections (150μm thick) containing the hippocampus were trimmed in cold artificial cerebrospinal fluid using a vibrotome (WT: n=5, WT/SCZ: n=7; TLR4 floxed SCZ: n=6 and TLR4 KD SCZ: n=6). Sections were rapidly fixed in 2% glutaraldehyde (warmed up to room temperature) and processed for osmium tetroxide staining as described previously by Schmidt et al. (2017). Ultrastructural images of the synapses were obtained using a transmission electron microscope (JEOL JEM-1011). Distribution of active synapses was determined by manual counting of post-synaptic densities at (X25,000). Diameter (nm) of post-synaptic density and membrane was measured at high magnification (X100,000).

Western blotting and protein quantification

For this procedure,15μl hippocampal lysate containing 15μg of protein was processed for SDS-PAGE electrophoresis (WT: n=10, WT/SCZ: n=10; TLR4 floxed SCZ: n=10 and TLR4 KD SCZ: n=10). After subsequent western blotting (wet transfer), Polyvinylidene fluoride membrane (PVDF) was incubated in Tris-buffered saline (with 0.01% Tween 20) for 15 minutes (TBST) at room temperature. Subsequently, immunoblot membrane was blocked in 3% bovine serum albumin (prepared in TBST) for 50 minutes at room temperature (25°C). The proteins of interest were detected using the following primary antibodies; Rabbit anti-PSD-95 (Cell Signaling-#3450S), Rabbit anti-GAPDH (Cell Signaling-#5174S), Rabbit anti-$GABA_BR$ (abcam-#ab166604), Rabbit anti-NMDAR (abcam-#ab17345), Rabbit anti-IGF-1R (Cell Signaling-#3027S), Rabbit anti-NF-κB (Thermofisher-#PA1-186), Mouse anti-TLR4 (abcam-#76B357.1), Mouse anti-CaMKIIα (Cell Signaling-#50049s), Mouse anti-SK2.2/KCNN2 (EMD Millipore-MABN1832), Rabbit anti-Phosphorylated CaMKIIα (Cell Signaling-#12716S), Rabbit anti-MAPK/ErK1/Erk2 (Cell Signaling-#9102S), Rabbit anti-Phosphorylated MAPK/ErK1/ErK2 (Cell Signaling-#4370S). All primary antibodies were diluted in blocking solution at 1:1,000. Subsequently, primary antibodies were detected using HRP-conjugated secondary antibodies [Goat anti Rabbit-#65-6120 and Goat anti-Mouse-#65-6520 (Invitrogen) at a dilution of 1: 5,000 or 1: 10,000. Subsequently, the reaction was developed using a chemiluminescent substrate (Thermofisher-#34579). Protein

expression was normalized per lane using the corresponding GAPDH and PSD-95 expression. Average normalized protein expression was determined and compared for WT and WT/SCZ groups in *T-Test*. Subsequently, all groups (WT, WT/SCZ, TLR4 floxed SCZ and TLR4 KD SCZ) were compared in *One-Way ANOVA* with Tukey *post-hoc* test. Statistical analysis was done in GraphPad Prism Version 7.0. Results were presented as bar chart with error bar representing Mean±SEM respectively.

Immunofluorescence

Animals were deeply anaesthetized with Isoflurane and perfused transcardially through the left ventricle using 10mM phosphate buffered saline (PBS). Subsequently, 4% phosphate buffered paraformaldehyde (PB-PFA) was introduced for perfusion fixation. Whole brain was excised through cranial dissection and fixed in 4% PB-PFA solution overnight, following which it was transferred to 4% PB-PFA containing 30% sucrose for cryopreservation. Free-floating cryostat sections (40μm) were obtained and preserved in 24-well plates containing 10mM PBS at 4°C (WT: n=15, WT/SCZ: n=20; TLR4 floxed SCZ: n=12 and TLR4 KD SCZ: n=15).

Sections were washed three times (5 Minutes each) in 10mM PBS (pH 7.4) on a tissue rocker. Subsequently, non-specific blocking was performed in normal goat serum (Vector Labs), prepared in 10mM PBS + 0.03% Triton-X100, for 2 hours at room temperature. Brain sections were incubated in primary antibody overnight at 4°C in primary antibody solution [Rabbit-anti IGF-1/IGF-1R (ThermoFisher; 1:250), Rabbit anti-MAPK/ErK1/ErK (Cell Signaling; 1:400), Mouse anti-CaMKIIα (Cell Signaling; 1:200), Rabbit anti-nNOS (Cell Signaling; 1:200), Mouse-anti-KCa2.2 (1:250; EMD Millipore-MABN1832), Anti-NeuN-Alexa 488 Conjugate (Millipore; 1:300), Guinea Pig anti-VGLUT 2 (EMD Millipore; 1:200), Rabbit anti-Tyrosine Hydroxylase, Rabbit anti-GABA (abcam; 1:200)] containing [10mMPBS+0.03% Triton-X 100 and normal goat serum]. Subsequently, sections were washed as previously described and incubated in secondary antibody solution [Goat anti-Rabbit or Mouse Alexa 568, Goat anti-Rabbit Alexa 594 and Goat anti-Guinea Pig Alexa 568 (diluted at 1:1000) prepared in 10mM PBS, 0.03% Triton X-100 and Normal Goat Serum] at room temperature (2 hours). Immunolabeled sections were washed and mounted on gelatin-coated slides using a plain or DAPI containing anti-fade mounting medium (Vector Labs).

Confocal Microscopy

Imaging of immunolabeled proteins in brain sections was done using a confocal laser scanner (Olympus FluoView 10i). To estimate neural Tyrosine hydroxylase, VGLUT2, GABA, CaMKIIα, IGF-1R, MAPK/ErK, and KCa2.2 expression we determined the threshold of normalized fluorescence intensity. Additionally, serology was done to determine the count of GFAP positive cells per unit area in brain slices. Determination of fluorescence intensity and cell count was done in Image J (NIH, USA) using methods previously described by Burges et al. (2010) and McCloy et al. (2014). For dendritic spine count per unit area, we used Image J and adopted the method previously described by Grishargin (2015). In all, fluorescence intensity and cell counting was done in *n=10* fields for *n=6* consecutive brain (serial) sections per animal. Average fluorescence intensity and cell count

was determined and compared for WT and WT/SCZ group in *T-Test*. Subsequently, all groups (WT, WT/SCZ, TLR4 floxed SCZ and TLR4 KD SCZ) were compared in *One-Way ANOVA* with Tukey *post-hoc* test. Statistical analysis was done in GraphPad Prism Version 7.0. Results were presented as bar chart with error bar representing Mean±SEM respectively.

Patch-Clamp Electrophysiology

Mice were decapitated after deep sedation with isoflurane. Whole brain was dissected and kept in ice-cold oxygenated artificial cerebrospinal fluid [aCSF; in mM 125 NaCl, 25 $NaHCO_3$, 3 KCl, 1.25 NaH_2PO_4, 1 $MgCl_2$, 2 $CaCl_2$ and 25 Glucose]. Coronal slices exposing the hippocampus (500μm thick) were obtained in cold oxygenated aCSF using a vibrotome and were immediately transferred into an oxygenated aCSF bath maintained at 34°C. After a recovery period of 1h, brain slices were transferred to a perfusion chamber mounted on the stage of an upright Olympus BX 51 Microscope (Olympus America, Center Valley, PA). Freshly aliquoted 3mg of Amphotericin B was dissolved in 50μl of dimethyl sulfonate (DMSO) and stored at −20°C. Subsequently, 8μl of Amphotericin B solution was added to 2ml of intracellular pipette solution (0.24mg/ml) [in mM 135 Potassium gluconate, 7 NaCl, 10 4-(2hydroxy ethyl)-1-piperazineethanesulfonic gluconate, 1–2 Na_2ATP, 0.3 Guanosine Trisphosphate (GTP) and $MgCl_2$; pH was adjusted with KOH and final Osmolality was set at 290mOsm] following which it was kept on ice and stored away from light. Flame pulled low resistance glass pipette electrode (3–5 MΩ) was prepared on a Flaming/Brown P-97 Micropipette puller (Stutter Instruments, Novato, CA) and filled with an intracellular solution containing Amphotericin B. Using a micromanipulator, a glass electrode was visually guided to the surface of a neuron following which negative pressure was applied to create a perforated patch. After 12–15 minutes, we isolated single-cell excitatory evoked potentials in current clamp mode. Only cells with access resistance of 5–20 MΩ were recorded (WT: n=5, WT/SCZ: n=10; TLR4 floxed SCZ: n=7 and TLR4 KD SCZ: n=6). Injected step currents were used to evoke changes to membrane potentials that were detected using a Multiclamp 700B Amplifier and Digidata 1440A digital acquisition system (Molecular Instruments). Analysis of recorded membrane potentials was done in ClampFit (Axon Instrument, Sunnyvale, CA). Frequency of action potential was determined and compared across all groups (WT, WT/SCZ, TLR4 floxed SCZ and TLR4 KD SCZ) in *One-Way ANOVA* with Tukey *post-hoc* test. Statistical analysis was done in GraphPad Prism Version 7.0. Results were presented as bar chart with error bar which represents the mean and standard error of mean respectively (Mean±SEM).

Results

Persistent NMDAR blockade caused social behavioral defects in WT mice

After an induced NMDAR hypofunction, we assessed behavioral change in pharmacologic mouse model of schizophrenia. Mice were tested in a social interaction chamber in order to evaluate sociability and social novelty behavior as illustrated in Fig. 2a. Using the scoring methods previously described by Kaidanovich-Beilin et al. (2011), schizophrenic animals show no preference for a strange mouse ($S1_a$) over an empty compartment (E) in the sociability chamber (sociability test) when compared with untreated WT mice (Fig. 2b; $p<0.01$). Similarly, in social novelty test, schizophrenic mice show no preference for a

second strange mouse (S2) over the first strange mouse ($S1_b$) when compared with WT (Fig. 2c; $p<0.01$).

Neurochemical characterization of NMDAR hypofunction model of schizophrenia

We measured corticostriatal tyrosine hydroxylase expression (fluorescence intensity) in behaviorally deficient schizophrenic mice through immunofluorescence and confocal microscopy. Tyrosine hydroxylase expression reduced significantly in dopaminergic neuronal projections in the prefrontal cortex (PFC) of behaviorally deficient mice in which we had previously induced NMDAR hypofunction (Fig. 2d–e; $p<0.05$). Conversely, there was a significant increase in striatal tyrosine hydroxylase positive terminals in behaviorally deficient schizophrenic mice (Fig. 2f–g; $p<0.01$). Going by the dopamine hypothesis of schizophrenia, our results show that pharmacologically induced NMDAR hypofunction can cause cortical hypodopaminergia and striatal hyperdopaminergia.

To determine the effect of induced NMDAR hypofunction on glutamatergic synaptic function, we measured the expression of vesicular glutamate transporter protein in the PFC of behaviorally deficient schizophrenic mice. The outcome demonstrates a significant decrease in cortical VGLUT2 expression after a persistent inhibition of brain NMDAR function (Fig. 2h–i). This outcome further supports occurrence of schizophrenic pathophysiology in our pharmacologic mouse model. In agreement with the glutamate hypothesis of schizophrenia, induced NMDAR hypofunction was linked to an abolished vesicular glutamate release in the cortex (Fig. 2h–i; $p<0.01$). In support of a significant change in neural function, we examined the distribution of inhibitory neurotransmitters - GABA – in the hippocampus of behaviorally deficient schizophrenic mice. Our results show a significant decrease in cortical GABA expression after an induced NMDAR hypofunction (Fig. 2j–k; $p<0.01$). Furthermore, GABAergic terminals appeared as clusters around scanty pyramidal neurons in Layer IV of the PFC. Since PFC GABAergic neurons are involved in the mitigation of learning and cognition (de Jonge et al., 2017; Nazakawa et al., 2017) our results suggest that induced NMDAR hypofunction may facilitate behavioral change in part by altering cortical GABAergic function. Therefore, ablation of NMDAR function altered behavior by modulating ionotropic neurotransmission involving Glutamatergic, GABAergic, and Dopaminergic neurons.

NMDAR hypofunction increased hippocampal pro-inflammatory signaling

In addition to a change in ionotropic neurotransmission, our results show a significant increase in pro-inflammatory proteins in the brain of schizophrenic mice in which we had previously blocked NMDAR activity. Based on our hypothesis, we anticipate that a change in synaptic NMDAR activity will be associated with increased inflammatory response that is linked with TLR4 signaling. In support of this proposition, our results show an increased TLR4 (Fig. 3a–b; $p<0.05$) and NF-κB expression (Fig. 3c–d; $p<0.05$) in hippocampal lysate of behaviorally deficient schizophrenic mice. Additionally, NF-κB expression significantly increased astrocyte-like cells in brain sections of schizophrenic mice ($p<0.01$) when compared with the control in immunofluorescence (Fig. 3e–f). Similarly, there was significant increase in GFAP positive cells (astrocyte) in the brain of schizophrenic mice when compared with the control ($p<0.01$; Fig. 3g–h). Together, our results show that an

induced NMDAR hypofunction can lead to behavioral defects of schizophrenia in part by mediating changes in neurotransmission and inflammatory response in the brain.

NMDAR hypofunction alters neural IGF-1R through upregulated MAPK/ErK

Consequent to an upregulated TLR4/NF-κB expression (inflammation) and defective neurotransmission in behaviorally deficient mice, we asked whether a persistent inhibition of NMDAR function can alter neurotropic receptor (IGF-1R) expression in the brain. In support of our hypothesis (Fig. 1), induced NMDAR hypofunction led to a significant loss of IGF-1R in the hippocampus of schizophrenic mice. This was evident in immunofluorescence ($p<0.001$; Fig. 4a–b) and immunoblot ($p<0.001$; Fig. 4c–d) quantification by which we compared hippocampal IGF-1R expression for control and schizophrenic mice.

To ascertain the relationship between upregulated TLR4/NF-κB, and IGF-1R depletion, we determined relative expression and phosphorylation of neural MAPK/ErK in the hippocampus of schizophrenic mice. In our hypothesis, we proposed that an upregulated TLR4 may significantly increase MAPK/ErK signaling through NF-κB-linked ErK activation. As such, an increased MAPK/ErK may consequently cause a decrease in IGF-1R signaling through negative regulation. The outcome of this aim laudably supports the proposition. Our results show that a decrease in IGF-1R expression was accompanied by a significant increase in hippocampal MAPK/ErK expression when assessed through immunofluorescence (Fig. 4e–f; $p<0.01$) and immunoblot quantification ($p<0.01$; Fig. 4g–h). Furthermore, we observed a significant increase in phosphorylated MAPK/ErK in hippocampal lysate of schizophrenic mice ($p<0.05$; Fig. 4i–j) when compared with the control. Thus, we inferred that induced NMDAR hypofunction can increase TLR4 signaling though upregulated NF-κB and phosphorylated (activated) MAP/ErK signaling. Furthermore, through increased MAPK/ErK activity, TLR4 may attenuate IGF-1R expression.

Loss of IGF-1R and increased TLR4 signaling led to a depletion of hippocampal CaMKIIα

Currently, our results show that induced NMDAR hypofunction modulates synaptic, inflammatory, and neurotropic changes that are associated with neural IGF-1R function. However, from our hypothesis, we are yet to determine whether induced NMDAR hypofunction can cause hippocampal CaMKIIα loss similar to IGF-1R. If this part of the hypothesis is valid, will TLR4 contribute to IGF-1R and CaMKIIα loss in NMDAR hypofunction-linked schizophrenia? Here, we show that a NMDAR hypofunction-linked IGF-1R depletion was also associated with a significant decrease in hippocampal CaMKIIα alpha expression as illustrated by immunofluorescence quantification (Fig. 5a–b). As such, behaviorally-deficient schizophrenic mice show a significant loss of CaMKIIα in the hippocampus when compared with the control ($p<0.001$). Additionally, we demonstrate a significant increase in CaMKIIα phosphorylation in hippocampal lysate of schizophrenic mice when compared with the control (Fig. 5c–d; $p<0.01$). This outcome supports our hypothesis (Fig. 1) as an increased NF-κB and pMAPK/ErK1/ErK1 can increase CaMKIIα loss through its phosphorylation (inactivation). Taken together, we infer that a change in NMDAR activity in the brain of behaviorally deficient schizophrenic mice may be an effect

of CaMKIIα loss that is mediated by MAPK/ErK activation which is associated with IGF-1R loss, and (or) an increased TLR4 signaling.

Tissue specific TLR4 knockdown in the hippocampus

To determine if a functional relationship exists between TLR4 signaling and attenuated IGF-1R/CaMKIIα activity, we created a hippocampal-specific TLR4 knockdown by expressing AAV-Cre in the hippocampus of TLR4 floxed mice (Fig. 6a–b). Equally, control TLR4 floxed mice express AAV-CMV-eGFP in the hippocampus and show no morphological difference when compared with WT (control) hippocampus (Fig. 6c–d). Expression of control and Cre-dependent viral vectors in neurons was verified by fluorescence imaging of reporter protein (eGFP; Fig. 6d). A successful TLR4 knockdown was further validated by immunoblot quantification of TLR4 in hippocampal lysate (Fig. 6e). As shown in Fig. 6f (bar graph), AAV-CMV-Cre expression in TLR4 floxed mice caused a significant decrease in hippocampal TLR4 expression ($p<0.01$).

TLR4 knockdown prevented NMDAR hypofunction-linked IGF-1R and CaMKIIα loss

After confirming TLR4 knockdown in the of hippocampus floxed mice, we induced NMDAR hypofunction as described previously for wild type mice. Interestingly, our result shows a sustained IGF-1R expression in the hippocampus of TLR4 KD SCZ mice when compared with WT expression in immunofluorescence (Fig. 7a–b) and western blots (Fig. 7c–d). Like the outcome for WT/SCZ mice, TLR4 floxed SCZ mice show a prominent loss of hippocampal IGF-1R when compared with WT (control; Fig. 7a–d). No significant change was recorded when we compared IGF-1R expression for TLR4 KD SCZ and untreated WT mice. Conversely, TLR4 floxed SCZ mice recorded a significant decrease in neural IGF-1R expression when compared with the control in immunofluorescence ($p<0.001$; Fig. 7a–b) and western blot ($p<0.001$; Fig. 7c–d).

In addition to preventing NMDAR hypofunction-linked IGF-1R loss, TLR4 knockdown attenuated MAPK/ErK expression in the hippocampus. As such, no significant change in MAPK/ErK was recorded in the hippocampus of TLR4 KD SCZ mice when compared with the control (Fig. 7e–f). Conversely, there was a significant increase in MAPK/ErK in the hippocampus of TLR4 floxed SCZ mice after an induced NMDAR hypofunction (Fig. 7e–f; $p<0.01$). In support of this outcome, there was no significant change for percentage phosphorylated MAPK/ErK in hippocampal lysate of TLR4 KD SCZ mice when compared with the control (Fig. 7g–h). However, percentage phosphorylated MAPK/ErK increased significantly for TLR4 floxed and WT mice after NMDAR hypofunction was induced ($p<0.05$; Fig. 7g–h).

Based on our hypothesis, a decrease in IGF-1R and increased TLR4 signaling may be associated with hippocampal CaMKIIα depletion in schizophrenia. Since TLR4 knockdown prevented IGF-1R loss, we asked whether a rescued IGF-1R signaling can prevent CaMKIIα loss after NMDAR hypofunction is induced. In addition to preventing IGF-1R loss, TLR4 knockdown attenuated hippocampal CaMKIIα loss that is linked to induced NMDAR hypofunction. As such, no significant change was observed when we compared hippocampal CaMKIIα expression for TLR4 KD SCZ and WT (control) mice (Fig. 8a–b; $p<0.001$).

Additionally, TLR4 knockdown attenuated CaMKIIα phosphorylation as shown in western blots (Fig. 8c–d). Versus WT/SCZ and TLR4 floxed SCZ, p-CaMKIIα was significantly lower after NMDAR hypofunction has been induced ($p<0.01$; Fig. 8c–d). As a confirmation of reduced neuronal TLR4 activity, there was no significant increase in NF-κB expression for TLR4 KD SCZ mice after NMDAR hypofunction is induced (Fig. 8e–f). Taken together, we deduce that hippocampal-specific TLR4 knockdown reduced NF-κB and MAPK/ErK signaling events that are associated with NMDAR hypofunction. As such, MAPK/ErK-mediated IGF-1R depletion and CaMKIIα phosphorylation were abolished (Fig. 8g).

TLR4 knockdown averted SCZ behavioral deficits linked with NMDAR hypofunction

Physiological implication of our results is further supported by behavioral test outcomes for TLR4 KD SCZ and TLR4 floxed mice. In spite of an induced NMDAR hypofunction, TLR4 KD SCZ mice recorded no significant change in social interaction behavior when compared with the control (Fig. 9a–c). In sociability and social novelty test, TLR4 KD SCZ mice exhibited a significant preference for $S1_a$ over E ($p<0.05$), and for S2 over $S1_b$ ($p<0.05$; Fig. 9a–c). However, TLR4 floxed SCZ mice recorded no significance in differential exploration time for $S1_a$/E or S2/$S1_b$ when compared with the WT/SCZ. Based on these outcomes, we infer that TLR4-mediated depletion of IGF-1R and CaMKIIα is a possible mechanism for synaptic dysfunction and behavioral abnormalities that is linked with NMDAR hypofunction-induced schizophrenia.

TLR4 knockdown prevented alterations in hippocampal synaptic function

As a confirmation of physiological change in synaptic function after NMDAR hypofunction and TLR4 knockdown, we evaluated frequency of evoked action potential in hippocampal neurons of WT, WT/SCZ, TLR4 floxed SCZ, and TLR4 KD SCZ mice. In behaviorally deficient schizophrenic mice (WT/SCZ and TLR4 floxed SCZ) there was a significant decrease in action potential when compared with the control ($p<0.001$; Fig. 9d–f). However, in TLR4 KD SCZ, no significant change in action potential was recorded in whole cell patch clamp recording; versus the control (Fig. 9d–e). Based on our hypothesis, in addition to modulation of NMDAR-dependent synaptic function, CaMKIIα regulates the activity of calcium activated potassium channels. In support of CaMKIIα-linked synaptic dysregulation, there was a significant increase in K+ after hyperpolarization currents in WT/SCZ and TLR4 floxed SCZ neurons when assessed in acute slice physiology. This may be associated with CaMKIIα loss or increased MAPK/ErK phosphorylation of pore-forming sub-units within these channels (i.e KCa.2.). To validate physiological dysregulation of CaMKIIα, there was a significant increase in hippocampal KCa2.2 expression when the channel was co-localized with PSD-95 in immunofluorescence. The most significant hippocampal KCa2.2 expression was seen in WT/SCZ ($p<0.001$) and TLR4 floxed SCZ ($p<0.01$; Fig. 10a–b) hippocampus versus the control. Since TLR knockdown rescued CaMKIIα loss, there was no significant change in KCa2.2 expression when we compared TLR4 KD SCZ mice with control (WT; Fig. 10a–b).

Other evidence supporting effectiveness of TLR4 knockdown as a tool to rescue synaptic dysfunction include a sustained NMDAR and $GABA_BR$ expression in the hippocampus of TLR4 KD SCZ mice when compared with the control (Fig. 10c–e). Conversely, WT/SCZ

and TLR4 floxed mice show a significant decrease in hippocampal NMDAR ($p<0.01$ and $p<0.05$) and GABA expression ($p<0.01$ and $p<0.01$) in the hippocampus after NMDAR hypofunction was induced (Fig. 10c–e)

TLR4 knockdown rescued changes in spine morphology

Using Golgi staining, we examined the morphology and count of dendritic spines on hippocampal neurons in the CA1-DG field (Fig. 11a–c). We found that both CA1 ($p<0.001$; Fig. 11a–b; $p<0.001$) and DG dendritic spines (Fig. 11a and Fig. 11c; $p<0.001$) were lost in the hippocampus of behaviorally deficient schizophrenic WT/SCZ and TLR4 floxed SCZ mice. Ultimately, in TLR4 knockdown mice (TLR4 KD SCZ) dendritic spine changes were significantly attenuated after an induced NMDAR hypofunction when compared with the control (Fig. 11a–c). In support of this outcome, all experimental SCZ group show a significant decrease in the thickness of post-synaptic densities when examined in TEM photomicrographs (Fig. 11d–e; $p<0.001$). However, threshold of PDS-95 loss was significantly attenuated in TLR4 KD SCZ mice when compared with WT/SCZ and TLR4 floxed SCZ groups ($p<0.05$; Fig. 11d–e). Taken together, we deduce that hippocampal-specific TLR4 knockdown can attenuate synaptic changes that are associated with NMDAR hypofunction induced schizophrenia.

Discussion

Pathophysiology of schizophrenia has long been perceived from “neurotransmitter imbalance” and “neurotransmitter receptor sensitivity” perspectives. Based on these school of thoughts, the dopamine hypothesis, and later a glutamate hypothesis of schizophrenia was proposed. These principles were also reflected in the treatment approach to schizophrenia. To date, most drugs available to treat schizophrenia target either dopamine and or glutamate receptors in the brain (Amodeo et al., 2017; Su et al., 2017). However, these treatment methods have been plagued with receptor sensitivity problems that may arise from prolonged use of antipsychotics like dopaminergic receptor antagonist (haloperidol) and glutamate receptor blocker (ketamine) (Ostinelli et al., 2017; Nikvarz et al., 2017). Recent advances in the study of schizophrenia now focus on the role of proteins that are associated with dysregulation of receptor function rather than the receptor itself.

Previous work by Yamasaki and colleagues demonstrated that genetic deletion of synaptic regulatory CaMKIIα caused synaptic and behavioral features of schizophrenia in mice (Yamasaki et al., 2008; Matsuo et al., 2009). CaMKIIα is important in schizophrenia because of its role in NMDAR function (Mao et al., 2014; Ma et al., 2015). Despite the several causes of schizophrenia (NIH-NIMH, 2017; SARDAA, 2017), loss of NMDAR function has been described as a unifying factor in disease progression (Balu et al., 2013; Balu and Coyle, 2014; Coyle, 2012; Dienel et al., 2017; Gao and Snyder, 2013). Since CaMKIIα facilitates the activity of NMDAR during long term potentiation (LTP) (Mao et al., 2014; Ma et al., 2015), we inferred that upstream receptors that can increase CaMKIIα activity might rescue NMDAR function in schizophrenia. Equally, upstream receptors that can reduce CaMKIIα function may promote NMDAR hypofunction that is associated with schizophrenia. Here, we identified IGF-1R (a neurotrophin receptor) and TLR4 (a

proinflammatory receptor) as potential non-neurotransmitter regulators of CaMKIIα function. While IGF-1R can increase CaMKIIα (Hu et al., 2016; Le Grevès et al., 2005; Dou et al., 2005), TLR4 can reduce CaMKIIα activity (Mémet, 2006; Kaltschmidt et al., 2005). However, how IGF-1R/TLR4 cross-talk in CaMKIIα function affects NMDAR activity in schizophrenia is poorly understood.

Taken together, the outcomes of this study show that induced NMDAR hypofunction is a cause of corticostriatal dopaminergic, glutamatergic and GABAergic changes which is required for characterization of disease model. Although CaMKIIα deletion is a cause of schizophrenia, here, we show that induced NMDAR hypofunction can facilitate hippocampal CaMKIIα loss in behaviorally deficient schizophrenia mice. Ultimately, we verified our hypothesis by confirming that NMDAR hypofunction-induced CaMKIIα loss involved IGF-1R depletion. Conversely, TLR4 knockdown prevented IGF-1R and CaMKIIα loss in mice after a persistent inhibition of NMDAR.

IGF-1R and TLR4 can regulate synaptic CaMKIIα

In our working model, we consider the synaptic regulatory activity of CaMKIIα in normal and schizophrenic synapses (Fig. 1). During normal synaptic function, CaMKIIα promotes NMDAR-linked calcium currents through NR sub-units of NMDAR (Mao et al., 2014; Ma et al., 2015). At the same time, CaMKIIα inhibits surrounding calcium-activated potassium channels (KCa2.2) by blocking the calcium-binding sites on the intracellular domain of the channel thereby preventing potassium efflux during an action potential (Allen et al., 2007; Dai et al., 2009; Lin et al., 2008). At the end of a synaptic potential, CaMKIIα phosphorylation by MAPK/ErK leads to its inactivation therefore terminating NMDAR-driven calcium current (Giovannini et al., 2001) and allowing KCa2.2-dependent K+ movement (Allen et al., 2007; Lin et al., 2008). This process, with contributions from AMPAR receptors, represents part of synchronous Ca^{2+}-K^{+} oscillation (Lisman and Zhabotinsky, 2001, Lisman et al., 2002).

Presynaptic IGF-1R can directly alter the LTP process through its effect on presynaptic calcium release and vesicle transport (Gazit et al., 2016). Additionally, post-synaptic IGF-1R contributes to kinase regulation of CaMKIIα (Gazit et al., 2016; Chiu and Cline, 2010). Therefore, factors that can cause a decrease in IGF-1R will reduce both presynaptic and post-synaptic function. Equally, a sustained and regulated IGF-1R signaling will preserve presynaptic vesicle transport and post-synaptic CaMKIIα function. By maintaining CaMKIIα function, a sustained IGF-1R expression will promote NMDAR function and inhibit KCa2.2 during LTP. However, an increased TLR4 signaling maintains NF-κB and MAPK/ErK (Venkatasubramanian and Debnath, 2013; García-Bueno et al., 2016; McKernan et al., 2011). Since both proteins can phosphorylate CaMKIIα, an increased TLR4 signaling can negatively regulate CaMKIIα expression and increase synaptic dysfunction in schizophrenia (Kéri et al., 2017). In addition to reducing CaMKIIα-linked NMDAR current, MAPK/ErK can also phosphorylate pore forming subunits of potassium channels (Barros et al., 2012; Gustina and Trudeau, 2011; Schrader et al., 2006; English and Sweatt; 1997; Selcher et al., 2003) thereby contributing to synaptic dysfunction.

To test our hypothesis on the mechanisms through which TLR4 and IGF-1R can putatively regulate synaptic CaMKIIα function, we characterized our model of schizophrenia using previously described behavioral and synaptic characteristics (Gao and Snyder, 2013; Nakata et al., 2017; Yamasaki et al., 2008; Matsuo et al., 2009; Kaidanovich-Beilin et al., 2011). After an induced NMDAR hypofunction in mice, there was significant loss of dendritic spine (Fig. 11a–c and Fig. 11d–e) and reduced synaptic potential (Fig. 9d–g) in hippocampal neurons. In addition to corticostriatal neurotransmitter changes (Fig. 2d–i), there was a significant dysregulation of glutamatergic (*VGLUT2:* Fig. 2h–i *NMDAR:* Fig. 10c–d) and GABAergic functions (*GABA:* Fig. 2j–k $GABA_BR$*:* Fig. 10c and Fig. 10e) in the brain schizophrenic mice. Furthermore, experimental animals were characterized by deficiencies in sociability and social novelty tests (Fig. 2a–c) similar to the observation for other experimental models of schizophrenia (Gao and Snyder, 2013; Becker, 2003; Yamasaki et al., 2008; Kaidanovich-Beilin et al., 2011).

CaMKIIα dysregulation is mediated through increased KCa2.2 activity in schizophrenia

Our results show that an induced NMDAR hypofunction is a cause of CaMKIIα and IGF-1R loss in the hippocampus of schizophrenic mice. In support of these outcomes, there was a significant reduction in synaptic potentials and increased after-hyperpolarization current that is linked with synaptic CaMKIIα dysfunction (Fig. 9d–f), and consequent upregulated KCa2.2 function (Fig. 10a–b). Based on our hypothesis, we deduced that increased neural TLR4 signaling contributed significantly to loss of CaMKIIα and IGF-1R after a persistent inhibition of NMDAR. As such, an increase in MAPK/ErK and NF-κB in schizophrenia can promote synaptic dysfunction through depletion of hippocampal IGF-1R and CaMKIIα. Ultimately, this may lead to a dysfunctional synaptic potential through loss of NMDAR-linked synaptic potentials, upregulated KCa2.2-mediated after-hyperpolarization effect.

Since CaMKIIα and MAPK are co-localized at PSDs (Giovannini et al., 2001; Tusi et al., 2005), we ask whether a change in MAPK phosphorylation of KCa2.2 was involved in the modulation of KCa2.2 function. Our results illustrate that an increase in MAPK/ErK was associated with increased KCa2.2 expression and AHP currents in the schizophrenic brain after NMDAR hypofunction was induced (Fig. 9a–b). Furthermore, in TLR4 knockdown hippocampus, there was a significant decrease in MAPK/ErK, KCa2.2 activity and AHP currents in patch clamping electrophysiology (Fig. 9d–f). As evidence of a change in post-synaptic function and morphology, a significant decrease in PSD thickness was recorded in ultrastructural analysis hippocampal synapses from behaviorally deficient schizophrenic mice (Fig. 11d–e). Interestingly, hippocampal-specific TLR4 knockdown attenuated changes in synaptic morphology that are associated with NMDAR hypofunction schizophrenia (Fig. 9, Fig. 10, Fig. 11a–e). Notably, as shown in Fig. 9d–f and Fig. 11d–e, loss of synaptic function and PSD were averted in the TLR4 KD SCZ mice when compared with WT/SCZ and TLR4 floxed mice. The physiological impact of TLR4 knockdown was ultimately assessed by evaluating social interaction behavior of the animals. WT and TLR4 floxed mice recorded significant defect in social interaction after an induced NMDAR hypofunction (Fig. 2a–c, Fig 9a–c). However, when NMDAR hypofunction was induced after TLR4 knockdown (TLR4 KD SCZ) the animals show no significant change in social interaction

behavior when compared with WT (control; Fig. 9a–c). These outcomes suggest a therapeutic significance for IGF-1R and TLR4-linked CaMKIIα signaling in schizophrenia.

TLR4 knockdown rescued IGF-1R/CaMKIIα expression in schizophrenia

Elements of the TLR4 signaling pathway have been shown to be upregulated in human schizophrenia and psychosis patients (McKernan et al., 2011; García-Bueno et al., 2016). The threshold of TLR4 signaling in schizophrenia is dependent on the use of antipsychotic agents and polymorphism in proteins associated with TLR4 receptor activation (García-Bueno et al., 2016). Our results demonstrate that induced NMDAR hypofunction can facilitate TLR4 signaling. Specifically, we identify the upregulation of MAPK/ErK and NF-κB as possible mechanisms through which TLR4 signaling may facilitate the progression of synaptic changes relative to NMDAR hypofunction schizophrenia.

Based on our results, some of the synaptic changes that may be attributable to increased TLR4 signaling in schizophrenia include: increased CaMKIIα phosphorylation by MAPK/ErK and NF-κB, dis-inhibition of KCa2.2 due to CaMKIIα phosphorylation, hyperactivation of KCa2.2 through MAPK-linked phosphorylation of its pore forming sub-unit, and downregulation of IGF-1R due to increased MAPK/ErK signaling downstream of TLR4. Consequently, decreased MAPK/ErK expression and phosphorylation are crucial to the mechanism through which TLR4 knockdown may prevent dysregulation of CaMKIIα and IGF-1R in the hippocampus of schizophrenic mice. Despite our progress, there are several areas of this interaction yet to be clarified. To date, it is unclear if IGF-1R signaling, is a cause or an effect of CaMKIIα loss in most schizophrenia mouse models. Furthermore, how TLR4 mediates NMDAR-linked IGF-1R and CaMKIIα loss is still poorly understood. There is a need for additional studies to determine if over expression of IGF-1R can be of therapeutic significance in schizophrenia. Furthermore, significance of this interaction needs to be investigated further in genetic models of schizophrenia.

Conclusions

We have shown the significance of TLR4 in upregulation of MAPK/ErK in NMDAR hypofunction schizophrenic-mouse model. This is characterized by a decrease in hippocampal IGF-1R/CaMKIIα, and social interaction behavioral deficits. Ultimately, hippocampal TLR4 knockdown rescued IGF-1R/CaMKIIα decline and prevented behavioral deficits by reducing MAPK/ErK expression.

Acknowledgments

This study was supported by the IBRO-ISN Fellowship 2015 awarded to OOM and Louisiana Board of Regents RCS Grant RD-A-09 and NIH/NIMH Grant R03 MH 104851 awarded to CCL.

References

1. Allen D, Fakler B, Maylie J, Adelman JP. Organization and Regulation of Small Conductance Ca2+-activated K+ Channel Multiprotein Complexes. The Journal of Neuroscience. 2007 Feb 28; 27(9): 2369–2376. [PubMed: 17329434]

2. Amodeo G, Fagiolini A, Sachs G, Erfurth A. Older and Newer Strategies for the Pharmacological Treatment of Agitation in Schizophrenia and Bipolar Disorder. CNS Neurol Disord Drug Targets. 2017 Sep 18.

3. Arain, Mariam, Haque, Maliha, Johal, Lina, Mathur, Puja, Nel, Wynand, Rais, Afsha, Sandhu, Ranbir, Sharma, Sushil. Maturation of the adolescent brain. Neuropsychiatric disease and treatment. 2013; 9(2013):449. [PubMed: 23579318]

4. Balu DT, Coyle JT. Chronic D-serine reverses arc expression and partially rescues dendritic abnormalities in a mouse model of NMDA receptor hypofunction. Neurochem Int. 2014 Sep.75:76–8. [PubMed: 24915645]

5. Balu DT, Li Y, Puhl MD, Benneyworth MA, Basu AC, Takagi S, Bolshakov VY, Coyle JT. Multiple risk pathways for schizophrenia converge in serine racemase knockout mice, a mouse model of NMDA receptor hypofunction. Proc Natl Acad Sci U S A. 2013 Jun 25; 110(26):E2400–9. [PubMed: 23729812]

6. Barkus C, Dawson LA, Sharp T, Bannerman DM. GluN1 hypomorph mice exhibit wide-ranging behavioral alterations. Genes Brain Behav. 2012 Apr; 11(3):342–51. [PubMed: 22300668]

7. Barros F, Domínguez P, de la Peña P. Cytoplasmic domains and voltage-dependent potassium channel gating. Front Pharmacol. 2012 Mar 23.3:49. [PubMed: 22470342]

8. Becker A, Peters B, Schroeder H, Mann T, Huether G, Grecksch G. Ketamine-induced changes in rat behaviour: A possible animal model of schizophrenia. Prog Neuropsychopharmacol Biol Psychiatry. 2003 Jun; 27(4):687–700. [PubMed: 12787858]

9. Burgess A, Vigneron S, Brioudes E, Labbé J-C, Lorca T, Castro A. Loss of human Greatwall results in G2 arrest and multiple mitotic defects due to deregulation of the cyclin B-Cdc2/PP2A balance. Proc Natl Acad Sci USA. 2010; 107:12564–12569. [PubMed: 20538976]

10. Cassilhas RC, Lee KS, Fernandes J, Oliveira MGM, Tufik S, Meeusen R, De Mello MT. Spatial memory is improved by aerobic and resistance exercise through divergent molecular mechanisms. Neuroscience. 2012; 202:309–317. [PubMed: 22155655]

11. Chang SH, Chiang SY, Chiu CC, Tsai CC, Tsai HH, Huang CY, Hsu TC, Tzang BS. Expression of anti-cardiolipin antibodies and inflammatory associated factors in patients with schizophrenia. Psychiatry research. 2011; 187(3):341–346. [PubMed: 20510460]

12. Chiu S, Cline HT. Insulin receptor signaling in the development of neuronal structure and function. Chiu and Cline Neural Development 2010. 2010; 5:7.a Cochrane Database Syst Rev. 2017 Sep 23.9:CD011831. [PubMed: 28940256]

13. Cohen SM, Tsien RW, Goff DC, Halassa MM. The impact of NMDA receptor hypofunction on GABAergic neurons in the pathophysiology of schizophrenia. Schizophr Res. 2015 Sep; 167(1–3): 98–107. [PubMed: 25583246]

14. Coyle JT. NMDA receptor and schizophrenia: a brief history. Schizophr Bull. 2012 Sep; 38(5): 920–6. [PubMed: 22987850]

15. Dai S, Hall DD, Hell JW. Supramolecular assemblies and localized regulation of voltage-gated ion channels. Physiol Rev. 2009 Apr; 89(2):411–52. DOI: 10.1152/physrev.00029.2007 [PubMed: 19342611]

16. de Jonge JC, Vinkers CH, Hulshoff Pol HE, Marsman A. GABAergic Mechanisms in Schizophrenia: Linking Postmortem and *In Vivo* Studies. Front Psychiatry. 2017 Aug 11.8:118. eCollection 2017. Review. doi: 10.3389/fpsyt.2017.00118 [PubMed: 28848455]

17. Demirel A, Demirel OF, Emül M, Duran A, Uğur M. Relationships between IGF-1, schizophrenia, and treatment of metabolic syndrome. Compr Psychiatry. 2014 Aug; 55(6):1391–7. [PubMed: 24850069]

18. Derkach VA, Oh MC, Guire ES, Soderling TR. Regulatory mechanisms of AMPA receptors in synaptic plasticity. Nat Rev Neurosci. 2007 Feb; 8(2):101–13. [PubMed: 17237803]

19. Dhavan R, Greer PL, Morabito MA, Orlando LR, Tsai LH. The cyclin-dependent kinase 5 activators p35 and p39 interact with the alpha-subunit of Ca2+/calmodulin-dependent protein kinase II and alpha-actinin-1 in a calcium-dependent manner. Neurosci. 2002 Sep 15; 22(18): 7879–91.

20. Dias AM. The Integration of the Glutamatergic and the White Matter Hypotheses of Schizophrenia's Etiology. Curr Neuropharmacol. 2012 Mar; 10(1):2–11. [PubMed: 22942875]

21. Dienel SJ, Bazmi HH, Lewis DA. Development of transcripts regulating dendritic spines in layer 3 pyramidal cells of the monkey prefrontal cortex: Implications for the pathogenesis of schizophrenia. Neurobiol Dis. 2017 Sep.105:132–141. [PubMed: 28576707]
22. Dou JT, Chen M, Dufour F, Alkon DL, Zhao WQ. Insulin receptor signaling in long-term memory consolidation following spatial learning. Learn Mem. 2005 Nov-Dec;12(6):646–55. [PubMed: 16287721]
23. Dou JT, Chen M, Dufour F, Alkon DL, Zhao WQ. Insulin receptor signaling in long-term memory consolidation following spatial learning. Learn Mem. 2005 Nov-Dec;12(6):646–55. [PubMed: 16287721]
24. Du J, Szabo ST, Gray NA, Manji HK. Focus on CaMKII: a molecular switch in the pathophysiology and treatment of mood and anxiety disorders. International Journal of Neuropsychopharmacology. 2004; 7(3):243–248. [PubMed: 15154976]
25. Dyer AH, Vahdatpour C, Sanfeliu A, Tropea D. The role of Insulin-Like Growth Factor 1 (IGF-1) in brain development, maturation and neuroplasticity. Neuroscience. 2016 Jun 14.325:89–99. [PubMed: 27038749]
26. Eckfeld A, Karlsgodt KH, Haut KM, Bachman P, Jalbrzikowski M, Zinberg J, van Erp TGM, Cannon TD, Bearden CE. Disrupted Working Memory Circuitry in Adolescent Psychosis. Front Hum Neurosci. 2017 Aug 8.11:394. [PubMed: 28848413]
27. English JD, Sweatt JD. A requirement for the mitogen-activated protein kinase cascade in hippocampal long term potentiation. J Biol Chem. 1997 Aug 1; 272(31):19103–6. [PubMed: 9235897]
28. Frankland PW, Sakaguchi M, Arruda-Carvalho M. Starting at the endophenotype: A role for alpha-CaMKII in schizophrenia? Mol Brain 2008. 2008 Sep 10.1:5.
29. Freyberg Z, Aslanoglou D, Shah R, Ballon JS. Intrinsic and Antipsychotic Drug-Induced Metabolic Dysfunction in Schizophrenia. Front Neurosci. 2017 Jul 28.11:432. [PubMed: 28804444]
30. Gao WJ, Snyder MA. NMDA hypofunction as a convergence point for progression and symptoms of schizophrenia. Front Cell Neurosci. 2013 Mar 27.7:31. [PubMed: 23543703]
31. García-Bueno B, Gassó P, MacDowell KS, Callado LF, Mas S, Bernardo M, Lafuente A, Meana JJ, Leza JC. Evidence of activation of the Toll-like receptor-4 proinflammatory pathway in patients with schizophrenia. J Psychiatry Neurosci. 2016 Apr; 41(3):E46–55. [PubMed: 27070349]
32. Gazit N, Vertkin I, Shapira I, Helm M, Slomowitz E, Sheiba M, Mor Y, Rizzoli S, Slutsky I. IGF-1R differentially regulates spontaneous and evoked transmission via mitochondria at hippocampal synapse. Neuron. 2016 Feb 3; 89(3):583–97. Epub 2016 Jan 21. DOI: 10.1016/j.neuron.2015.12.034 [PubMed: 26804996]
33. Giovannini MG, Blitzer RD, Wong T, Asoma K, Tsokas P, Morrison JH, Iyengar R, Landau EM. Mitogen-Activated Protein Kinase Regulates Early Phosphorylation and Delayed Expression of Ca2+/Calmodulin-Dependent Protein Kinase II in Long-Term Potentiation. The Journal of Neuroscience. 2001 Sep 15; 21(18):7053–7062. [PubMed: 11549715]
34. Gómez-Villafuertes R, García-Huerta P, Díaz-Hernández JI, Miras-Portugal MT. PI3K/Akt signaling pathway triggers P2X7 receptor expression as a pro-survival factor of neuroblastoma cells under limiting growth conditions. Scientific reports. 2015:5.
35. Grishagin IV. Automatic cell counting with ImageJ. Anal Biochem. 2015 Mar 15.473:63–5. Epub 2014 Dec 24. DOI: 10.1016/j.ab.2014.12.007 [PubMed: 25542972]
36. Gunnell D, Lewis S, Wilkinson J, Georgieva L, Davey GS, Day IN, Holly JM, O'Donovan MC, Owen MJ, Kirov G, Zammit. IGF1, growth pathway polymorphisms and schizophrenia: a pooling study. Am J Med Genet B Neuropsychiatr Genet. 2007 Jan 5; 144B(1):117–20. [PubMed: 17044098]
37. Gustina AS, Trudeau MC. hERG potassium channel gating is mediated by N- and C-terminal region interactions. J Gen Physiol. 2011 Mar; 137(3):315–25. [PubMed: 21357734]
38. Hagihara H, Shoji H, Takao K, Walton NM, Matsumoto M, Miyakawa T. Immaturity of brain as an endophenotype of neuropsychiatric disorders. Nihon Shinkei Seishin Yakurigaku Zasshi. 2014 Jun; 34(3):67–79. [PubMed: 25076776]

39. Hagihara H, Takao K, Walton NM, Matsumoto M, Miyakawa T. Immature dentate gyrus: an endophenotype of neuropsychiatric disorders. Neural Plast. 2013; 2013:318596. [PubMed: 23840971]
40. Hami J, Kheradmand H, Haghir H. Gender differences and lateralization in the distribution pattern of insulin-like growth factor-1 receptor in developing rat hippocampus: an immunohistochemical study. Cell Mol Neurobiol. 2014 Mar; 34(2):215–26. [PubMed: 24287499]
41. Han SJ, Lonard DM, O'Malley BW. Multi-modulation of nuclear receptor coactivators through posttranslational modifications. Trends in Endocrinology & Metabolism. 2009; 20(1):8–15. [PubMed: 19019695]
42. Hansen T, Jakobsen KD, Fenger M, Nielsen J, Krane K, Fink-Jensen A, Lublin H, Ullum H, Timm S, Wang AG, Jørgensen NR, Werge T. Variation in the purinergic P2RX7 receptor gene and schizophrenia. Schizophrenia research. 2008; 104(1):146–152. [PubMed: 18614336]
43. Henneberger C, Steinhäuser C. Astrocytic TLR4 at the crossroads of inflammation and seizure susceptibility. J Cell Biol. 2016 Dec 5; 215(5):607–609. [PubMed: 27881712]
44. Howes OD, McCutcheon R, Owen MJ, Murray RM. The Role of Genes, Stress, and Dopamine in the Development of Schizophrenia. Biol Psychiatry. 2017 Jan 1; 81(1):9–20. [PubMed: 27720198]
45. Hu A, Yuan H, Wu L, Chen R, Chen Q, Zhang T, Wang Z, Liu P, Zhu X. The effect of constitutive over-expression of insulin-like growth factor 1 on the cognitive function in aged mice. Brain Res. 2016 Jan 15.1631:204–13. [PubMed: 26581336]
46. Hu A, Yuan H, Wu L, Chen R, Chen Q, Zhang T, Wang Z, Liu P, Zhu X. The effect of constitutive over-expression of insulin-like growth factor 1 on the cognitive function in aged mice. Brain Res. 2016 Jan 15.1631:204–13. [PubMed: 26581336]
47. Hu A, Yuan H, Wu L, Chen R, Chen Q, Zhang T, Wang Z, Liu P, Zhu X. The effect of constitutive over-expression of insulin-like growth factor 1 on the cognitive function in aged mice. Brain Research. 2016; 1631:204–213. [PubMed: 26581336]
48. Huang W, Ghisletti S, Perissi V, Rosenfeld MG, Glass CK. Transcriptional integration of TLR2 and TLR4 signaling at the NCoR derepression checkpoint. Molecular cell. 2009; 35(1):48–57. [PubMed: 19595715]
49. Ibi D, de la Fuente Revenga M, Kezunovic N, Muguruza C, Saunders JM, Gaitonde SA, Moreno JL, Ijaz MK, Santosh V, Kozlenkov A, Holloway T, Seto J, García-Bea A, Kurita M, Mosley GE, Jiang Y, Christoffel DJ, Callado LF, Russo SJ, Dracheva S, López-Giménez JF, Ge Y, Escalante CR, Meana JJ, Akbarian S, Huntley GW, González-Maeso J. Antipsychotic-induced Hdac2 transcription via NF-κB leads to synaptic and cognitive side effects. Nat Neurosci. 2017 Sep; 20(9):1247–1259. [PubMed: 28783139]
50. Jiang G, Wang W, Cao Q, Gu J, Mi X, Wang K, Chen G, Wang X. Insulin growth factor-1 (IGF-1) enhances hippocampal excitatory and seizure activity through IGF-1 receptor-mediated mechanisms in the epileptic brain. Clin Sci (Lond). 2015 Dec; 129(12):1047–60. Epub 2015 Aug 18. DOI: 10.1042/CS20150312 [PubMed: 26286172]
51. Johnston HM, Morris BJ. N-methyl-D-aspartate and nitric oxide regulate the expression of calcium/calmodulin-dependent kinase II in the hippocampal dentate gyrus. Brain Res Mol Brain Res. 1995 Jul; 31(1–2):141–50. [PubMed: 7476022]
52. Kaidanovich-Beilin O, Lipina T, Vukobradovic I, Roder J, Woodgett JR. Assessment of Social Interaction Behaviors. 2011Pereira C, Schaer DJ, Bachli EB, Kurrer MO, Schoedon G. J Vis Exp. 2011; (48):e2473.
53. Kaltschmidt B, Widera D, Kaltschmidt C. Signaling via NF-kappaB in the nervous system. Biochim Biophys Acta. 2005 Sep 30; 1745(3):287–99. [PubMed: 15993497]
54. Kaltschmidt B, Widera D, Kaltschmidt C. Signaling via NF-kappaB in the nervous system. Biochim Biophys Acta. 2005 Sep 30; 1745(3):287–99. [PubMed: 15993497]
55. Kéri S, Seres I, Kelemen O, Benedek G. The relationship among neuregulin 1-stimulated phosphorylation of AKT, psychosis proneness, and habituation of arousal in nonclinical individuals. Schizophr Bull. 2011 Jan; 37(1):141–7. [PubMed: 19549627]
56. Kéri S, Szabó C, Kelemen O. Uniting the neuro developmental and immunological hypotheses: Neuregulin 1 receptor ErbB and Toll-like receptor activation in first-episode schizophrenia. Sci Rep. 2017 Jun 23.7(1):4147. [PubMed: 28646138]

57. Kiray M, Sisman AR, Camsari UM, Evren M, Dayi A, Baykara B, Aksu I, Ates M, Uysal N. Effects of carbon dioxide exposure on early brain development in rats. Biotech Histochem. 2014 Jul; 89(5):371–83. Epub 2014 Jan 29. DOI: 10.3109/10520295.2013.872298 [PubMed: 24476563]
58. Le Grevès M, Le Grevès P, Nyberg F. Age-related effects of IGF-1 on the NMDA-, GH- and IGF-1-receptor mRNA transcripts in the rat hippocampus. Brain Res Bull. 2005 May 15; 65(5): 369–74. [PubMed: 15833590]
59. Le Grevès M, Le Grevès P, Nyberg F. Age-related effects of IGF-1 on the NMDA-, GH- and IGF-1-receptor mRNA transcripts in the rat hippocampus. Brain Res Bull. 2005 May 15; 65(5): 369–74. [PubMed: 15833590]
60. Le Grevès M, Le Grevès P, Nyberg F. Age-related effects of IGF-1 on the NMDA-, GH- and IGF-1-receptor mRNA transcripts in the rat hippocampus. Brain Res Bull. 2005 May 15; 65(5): 369–74. [PubMed: 15833590]
61. Le Grevès M, Zhou Q, Berg M, Le Grevès P, Fhölenhag K, Meyerson B, Nyberg F. Growth hormone replacement in hypophysectomized rats affects spatial performance and hippocampal levels of NMDA receptor subunit and PSD-95 gene transcript levels. Exp Brain Res. 2006 Aug; 173(2):267–73. [PubMed: 16633806]
62. Lin MT, Luján R, Watanabe M, Adelman JP, Maylie J. SK2 channel plasticity contributes to LTP at Schaffer collateral–CA1 synapses. Nature neuroscience. 2008; 11(2):170–177. [PubMed: 18204442]
63. Lisman JE, Zhabotinsky AM. A model of synaptic memory: a CaMKII/PP1 switch that potentiates transmission by organizing an AMPA receptor anchoring assembly. Neuron. 2001; 31(2):191–201. [PubMed: 11502252]
64. Lisman J, Schulman H, Cline H. The molecular basis of CaMKII function in synaptic and behavioural memory. Nature Reviews Neuroscience. 2002; 3(3):175–190. [PubMed: 11994750]
65. Luo F, Yang C, Chen Y, Shukla P, Tang L, Wang LX, Wang ZJ. Reversal of chronic inflammatory pain by acute inhibition of Ca2+/calmodulin-dependent protein kinase II. Journal of Pharmacology and Experimental Therapeutics. 2008; 325(1):267–275. [PubMed: 18178903]
66. Ma J, Duan Y, Qin Z, Wang J, Liu W, Xu M, Zhou S, Cao X. Overexpression of αCaMKII impairs behavioral flexibility and NMDAR-dependent long-term depression in the medial prefrontal cortex. Neuroscience. 2015 Dec 3.310:528–40. [PubMed: 26415772]
67. Mao LM, Jin DZ, Xue B, Chu XP, Wang JQ. Phosphorylation and regulation of glutamate receptors by CaMKII. Sheng Li Xue Bao. 2014 Jun 25; 66(3):365–72. [PubMed: 24964855]
68. Matsuo N, Yamasaki N, Ohira K, Takao K, Toyama K, Eguchi M, Yamaguchi S, Miyakawa T. Neural activity changes underlying the working memory deficit in alpha-CaMKII heterozygous knockout mice. Front Behav Neurosci. 2009 Sep 2.3:20. [PubMed: 19750198]
69. McCloy RA, Rogers S, Caldon CE, Lorca T, Castro A, Burgess A. Partial inhibition of Cdk1 in G 2 phase overrides the SAC and decouples mitotic events. Cell Cycle. 2014; 13:1400–1412. [PubMed: 24626186]
70. McKernan DP, Dennison U, Gaszner G, Cryan JF, Dinan TG. Enhanced peripheral toll-like receptor responses in psychosis: further evidence of a pro-inflammatory phenotype. Transl Psychiatry. 2011 Aug 30.1:e36.doi: 10.1038/tp.2011.37 [PubMed: 22832610]
71. McQuillin A, Bass NJ, Choudhury K, Puri V, Kosmin M, Lawrence J, Curtis D, Gurling HM. Case–control studies show that a non-conservative amino-acid change from a glutamine to arginine in the P2RX7 purinergic receptor protein is associated with both bipolar-and unipolar-affective disorders. Molecular psychiatry. 2009; 14(6):614–620. [PubMed: 18268501]
72. Meffert MK, Baltimore D. Physiological functions for brain NF-κB. Trends in neurosciences. 2005; 28(1):37–43. [PubMed: 15626495]
73. Meltzer HY. New Trends in the Treatment of Schizophrenia. CNS Neurol Disord Drug Targets. 2017 Jul 28.
74. Mémet S. NF-kappaB functions in the nervous system: from development to disease. Biochem Pharmacol. 2006 Oct 30; 72(9):1180–95. [PubMed: 16997282]
75. Mémet S. NF-kappaB functions in the nervous system: from development to disease. Biochem Pharmacol. 2006 Oct 30; 72(9):1180–95. [PubMed: 16997282]

76. Nakata Y, Kanahara N, Iyo M. Dopamine supersensitivity psychosis in schizophrenia: Concepts and implications in clinical practice. J Psychopharmacol. 2017 Sep.1:269881117728428.
77. Nakazawa K, Jeevakumar V, Nakao K. Spatial and temporal boundaries of NMDA receptor hypofunction leading to schizophrenia. NPJ Schizophr. 2017 Feb 3.3:7. [PubMed: 28560253]
78. Nelson PG, Kuddo T, Song EY, Dambrosia JM, Kohler S, Satyanarayana G, Vandunk C, Grether JK, Nelson KB. Selected neurotrophins, neuropeptides, and cytokines: developmental trajectory and concentrations in neonatal blood of children with autism or Down syndrome. International journal of developmental neuroscience. 2006; 24(1):73–80. [PubMed: 16289943]
79. Netchine I, Azzi S, Le Bouc Y, Savage MO. IGF1 molecular anomalies demonstrate its critical role in fetal, postnatal growth and brain development. Best Pract Res Clin Endocrinol Metab. 2011 Feb; 25(1):181–90. [PubMed: 21396584]
80. Ng J, Rashid AJ, So CH, O'Dowd BF, George SR. Activation of calcium/calmodulin-dependent protein kinase IIalpha in the striatum by the heteromeric D1–D2 dopamine receptor complex. Neuroscience. 2010 Jan 20; 165(2):535–41. [PubMed: 19837142]
81. NIH-NIMH: National Institute of Mental Health. Schizophrenia; statistics and prevalence. 2017. https://www.nimh.nih.gov/health/statistics/prevalence/schizophrenia.shtml
82. Nikvarz N, Vahedian M, Khalili N. Chlorpromazine versus penfluridol for schizophrenia. 2017
83. Ostinelli EG, Brooke-Powney MJ, Li X, Adams CE. Haloperidol for psychosis-induced aggression or agitation (rapid tranquillisation). Cochrane Database Syst Rev. 2017 Jul 31.7:CD009377. [PubMed: 28758203]
84. Owen MJ, O'Donovan MC. Schizophrenia and the neurodevelopmental continuum:evidence from genomics. World Psychiatry. 2017 Oct; 16(3):227–235. (2012). [PubMed: 28941101]
85. Owens SJ, Murphy CE, Purves-Tyson TD, Weickert TW, Shannon Weickert C. Considering the role of adolescent sex steroids in schizophrenia. J Neuroendocrinol. 2017 Sep 23. (2012).
86. Park CS, Elgersma Y, Grant SG, Morrison JH. alpha-Isoform of calcium-calmodulin-dependent protein kinase II and postsynaptic density protein 95 differentially regulate synaptic expression of NR2A- and NR2B-containing N-methyl-d-aspartate receptors in hippocampus. Neuroscience. 2008 Jan 2; 151(1):43–55. [PubMed: 18082335]
87. Pereira C, Schaer DJ, Bachli EB, Kurrer MO, Schoedon G. Wnt5A/CaMKII signaling contributes to the inflammatory response of macrophages and is a target for the antiinflammatory action of activated protein C and interleukin-10 (2008). Arterioscler Thromb Vasc Biol. 2008 Mar; 28(3): 504–10. [PubMed: 18174455]
88. Purkayastha S, Ford J, Kanjilal B, Diallo S, Del Rosario Inigo J, Neuwirth L, El Idrissi A, Ahmed Z, Wieraszko A, Azmitia EC, Banerjee P. Clozapine functions through the prefrontal cortex serotonin 1A receptor to heighten neuronal activity via calmodulin kinase II-NMDA receptor interactions. J Neurochem. 2012 Feb; 120(3):396–407. [PubMed: 22044428]
89. Purves-Tyson TD, Owens SJ, Rothmond DA, Halliday GM, Double KL, Stevens J, McCrossin T, Shannon Weickert C. Putative presynaptic dopamine dysregulation in schizophrenia is supported by molecular evidence from post-mortem human midbrain. Transl Psychiatry. 2017 Jan 17.7(1):e1003. [PubMed: 28094812]
90. Ribasés M, Hervás A, Ramos-Quiroga JA, Bosch R, Bielsa A, Gastaminza X, Fernández-Anguiano M, Nogueira M, Gómez-Barros N, Valero S, Gratacòs M, Estivill X, Casas M, Cormand B, Bayés M. Association study of 10 genes encoding neurotrophic factors and their receptors in adult and child attention-deficit/hyperactivity disorder. Biological psychiatry. 2008; 63(10):935–945. [PubMed: 18179783]
91. Robison AJ, Bass MA, Jiao Y, MacMillan LB, Carmody LC, Bartlett RK, Colbran RJ. Multivalent interactions of calcium/calmodulin-dependent protein kinase II with the postsynaptic density proteins NR2B, densin-180, and alpha-actinin-2. J Biol Chem. 2005 Oct 21; 280(42):35329–36. [PubMed: 16120608]
92. Romanelli RJ, LeBeau AP, Fulmer CG, Lazzarino DA, Hochberg A, Wood TL. Insulin-like growth factor type-I receptor internalization and recycling mediate the sustained phosphorylation of Akt. J Biol Chem. 2007 Aug 3; 282(31):22513–24. [PubMed: 17545147]

93. Salani B, Ravera S, Amaro A, Salis A, Passalacqua M, Millo E, Damonte G, Marini C, Pfeffer U, Sambuceti G, Cordera R, Maggi D. IGF1 regulates PKM2 function through Akt phosphorylation. Cell Cycle. 2015; 14(10):1559–67. DOI: 10.1080/15384101.2015.1026490 [PubMed: 25790097]
94. SARDAA: Schizophrenia and Related Disorders Alliance of America. About Schizophrenia. 2017. https://sardaa.org/resources/about-schizophrenia/
95. Schmidt H, Gour A, Straehle J, Boergens KM, Brecht M, Helmstaedter M. Axonal synapse sorting in medial entorhinal cortex. Nature. 2017 Sep 28; 549(7673):469–475. Epub 2017 Sep 20. DOI: 10.1038/nature24005 [PubMed: 28959971]
96. Schrader LA, Birnbaum SG, Nadin BM, Ren Y, Bui D, Anderson AE, Sweatt JD. ERK/MAPK regulates the Kv4.2 potassium channel by direct phosphorylation of the pore-forming subunit. Am J Physiol Cell Physiol. 2006 Mar; 290(3):C852–61. [PubMed: 16251476]
97. Seillier A, Giuffrida A. Evaluation of NMDA receptor models of schizophrenia: divergences in the behavioral effects of sub-chronic PCP and MK-801. Behav Brain Res. 2009 Dec 7; 204(2):410–5. [PubMed: 19716985]
98. Selcher JC, Weeber EJ, Christian J, Nekrasova T, Landreth GE, Sweatt JD. A role for ERK MAP kinase in physiologic temporal integration in hippocampal area CA1. Learn Mem. 2003 Jan-Feb; 10(1):26–39. [PubMed: 12551961]
99. Shen Y, Qin H, Chen J, Mou L, He Y, Yan Y, Zhou H, Lv Y, Chen Z, Wang J, Zhou YD. Postnatal activation of TLR4 in astrocytes promotes excitatory synaptogenesis in hippocampal neurons. J Cell Biol. 2016 Dec 5; 215(5):719–734. [PubMed: 27920126]
100. Su YA, Yan F, Li Q, Xiang YT, Shu L, Yu X, Ning YP, Zhang KR, Li T, Mei QY, Li KQ, Si TM. Anticholinergic use trends in 14,013 patients with schizophrenia from three national surveys on the use of psychotropic medications in China (2002–2012). Psychiatry Res. 2017 Jul 21.257:132–136. [PubMed: 28755603]
101. Sun LY. Hippocampal IGF-1 expression, neurogenesis and slowed aging: clues to longevity from mutant mice. Age (Dordr). 2006 Jun; 28(2):181–9. [PubMed: 19943139]
102. Takeuchi Y, Fukunaga K, Miyamoto E. Activation of nuclear Ca(2+)/calmodulin-dependent protein kinase II and brain-derived neurotrophic factor gene expression by stimulation of dopamine D2 receptor in transfected NG108–15 cells. J Neurochem. 2002 Jul; 82(2):316–28. [PubMed: 12124432]
103. Tsui J, Inagaki M, Schulman H. Calcium/calmodulin-dependent protein kinase II (CaMKII) localization acts in concert with substrate targeting to cr eate spatial restriction for phosphorylation. J Biol Chem. 2005 Mar 11; 280(10):9210–6. Epub 2004 Dec 6. [PubMed: 15582994]
104. Vahdatpour C, Dyer AH. Tropea DInsulin-Like Growth Factor 1 and Related Compounds in the Treatment of Childhood-Onset Neurodevelopmental Disorders. Front Neurosci. 2016 Sep 30.10:450. eCollection 2016. [PubMed: 27746717]
105. Vekshina NL, Anokhin PK, Veretinskaya AG, Shamakina IY. Heterodimeric D1D2 dopamine receptors: a review. Biomed Khim. 2017 Jan; 63(1):5–12. [PubMed: 28251946]
106. Venkatasubramanian G, Chittiprol S, Neelakantachar N, Shetty T, Gangadhar BN. Effect of antipsychotic treatment on Insulin-like Growth Factor-1 and cortisol in schizophrenia: a longitudinal study. Schizophr Res. 2010 Jun; 119(1–3):131–7. Epub 2010 Mar 11. DOI: 10.1016/j.schres.2010.01.033 [PubMed: 20226630]
107. Venkatasubramanian G, Debnath M. The TRIPS (Toll-like receptors in immuno-inflammatory pathogenesis) Hypothesis: a novel postulate to understand schizophrenia. Progress in Neuro-Psychopharmacology and Biological Psychiatry. 2013; 44:301–311. [PubMed: 23587629]
108. Xing L, Larsen RS, Bjorklund GR, Li X, Wu Y, Philpot BD, Snider WD, Newbern JM. Layer specific and general requirements for ERK/MAPK signaling in the developing neocortex. eLife. 2016; 5:e11123. [PubMed: 26848828]
109. Yamasaki N, Maekawa M, Kobayashi K, Kajii Y, Maeda J, Soma M, Takao K, Tanda K, Ohira K, Toyama K, Kanzaki K, Fukunaga K, Sudo Y, Ichinose H, Ikeda M, Iwata N, Ozaki N, Suzuki H, Higuchi M, Suhara T, Yuasa S, Miyakawa T. Alpha-CaMKII deficiency causes immature dentate gyrus, a novel candidate endophenotype of psychiatric disorders. Mol Brain. 2008 Sep 10.1:6. [PubMed: 18803808]

110. Yang AC, Tsai SJ. New Targets for Schizophrenia Treatment beyond the Dopamine Hypothesis. Int J Mol Sci. 2017 Aug 3.18(8)

111. Zheng W, Wang H, Zeng Z, Lin J, Little PJ, Srivastava LK, Quirion R. The possible role of the Akt signaling pathway in schizophrenia. Brain Res. 2012 Aug 27.1470:145–58. [PubMed: 22771711]

Highlights

- Induced NMDAR hypofunction caused hippocampal CaMKIIα loss.
- Depletion of hippocampal IGF-1R was linked with CaMKIIα loss in NMDAR hypofunction.
- *Cre-lox* knockdown of TLR4 rescued IGF-1R and CaMKIIα loss after an induced NMDAR hypofunction.

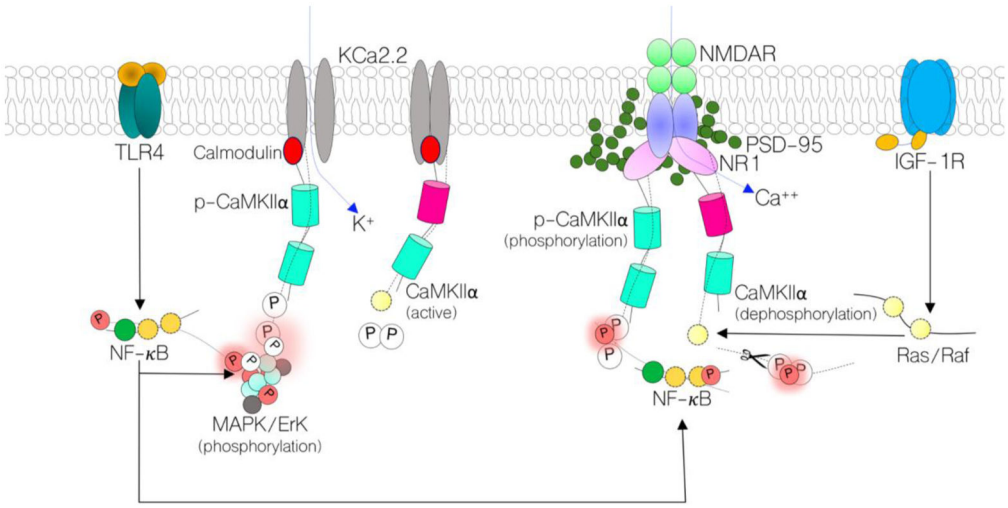

Figure 1.

Schematic illustration of the proposed mechanism through which TLR4 and IGF-1R signaling can alter the activity of synaptic CaMKIIα. Through *Ras/Raf* signaling, IGF-1R can upregulate the activity of CaMKIIα thereby increasing NMDAR-linked Ca^{2+} current at post-synaptic densities. Additionally, activated CaMKIIα can block the Ca^{2+} binding sites on surrounding calcium-activated potassium channels (KCa2.2). The physiological impact of IGF-1R-mediated CaMKIIα function is a sustained synaptic function (synaptic potentiation). Conversely, increased TLR4 signaling can increase NF-κB and MAPK/ErK activity: both of which can phosphorylate (inactivate) CaMKIIα relative to synaptic function and inflammation. Equally, MAPK/ErK can phosphorylate the pore forming subunits of KCa2.2 leading to an increase in K^+ influx, and attenuated synaptic potential (synaptic depression). In hippocampal-specific TLR4 knockdown, we anticipate a reduced MAPK/ErK and NF-κB activity. Ultimately, when NMDAR hypofunction is induced, CaMKIIα loss will be averted – in part – to prevent total synaptic dysfunction. Therefore, NMDAR hypofunction and IGF-1R loss may be reversed in behaviorally deficient schizophrenia mice.

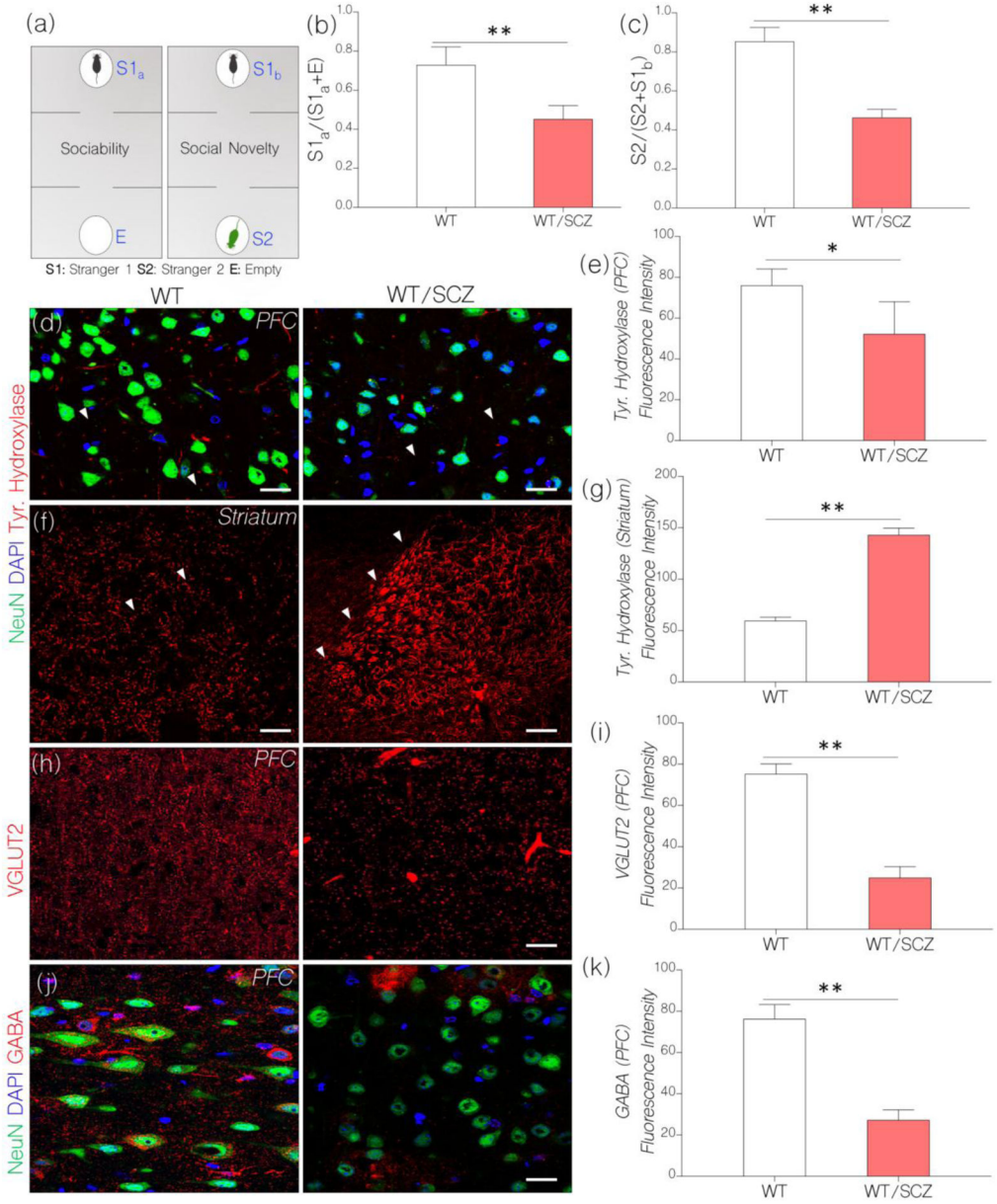

Figure 2.

a, Diagrammatic illustration of the steps involved in the behavioral test paradigm for assessing social behavior after NMDAR hypofunction has been induced in mice. The test involves two separate phases: sociability test and social novelty test.

b, Bar chart depicting sociability test outcome in control and NMDAR hypofunction mice. Induced NMDAR hypofunction caused a decline in sociability behavior in WT mice treated with ketamine (WT/SCZ). WT/SCZ mice showed no preference for stranger 1 ($S1_a$) versus the empty chamber "E" (n=10) when compared with the control ($p<0.01$).

c, Social Novelty: WT/SCZ mice showed no preference for *S2* over $S1_b$ (n=10). As such, WT/SCZ group was considered deficient in social novelty when compared with the control ($p<0.01$).

d, Representative confocal images show a change in cortical tyrosine hydroxylase in behaviorally deficient mice after induced NMDAR hypofunction. Induced NMDAR hypofunction caused a decrease in tyrosine hydroxylase positive terminals in the PFC when compared with the control ($p<0.05$; scale bar=20μm). Arrow heads indicate tyrosine hydroxylase positive terminals in the PFC.

e, Bar chart depicting statistical comparison for cortical tyrosine hydroxylase expression in WT (control) and NMDAR hypofunction (WT/SCZ) PFC.

f, Representative confocal images show a change in striatal tyrosine hydroxylase expression after induced NMDAR hypofunction. WT/SCZ mice exhibited striatal hyperdopaminergia when compared with the control ($p<0.01$; scale bar=40μm). Arrow heads highlight the margin of tyrosine hydroxylase fibers within the striatum.

g, Bar chart illustrating the expression of striatal tyrosine hydroxylase for WT and WT/SCZ group.

h, Confocal images show vesicular glutamate transporter (VGLUT2) expression in the cortex. After induced NMDAR hypofunction (WT/SCZ), VGLUT2 expression decreased significantly in the PFC when compared with the control ($p<0.01$; scale bar=20μm).

i, Bar chart show a reduction in VGLUT2 expression in the PFC of WT/SCZ mice: versus the control.

j, Confocal images show a combined localization of GABA and neuron (NeuN) in the PFC. Cortical GABA expression reduced significantly in mice after an induced NMDAR hypofunction ($p<0.01$ versus the control). GABA positive neuronal clusters formed enlarged patches around neuronal cell bodies in the PFC of WT/SCZ mice (scale bar=20μm).

k, Bar graph demonstrating statistical comparison for GABA expression in the PFC of control (WT) and WT/SCZ mice.

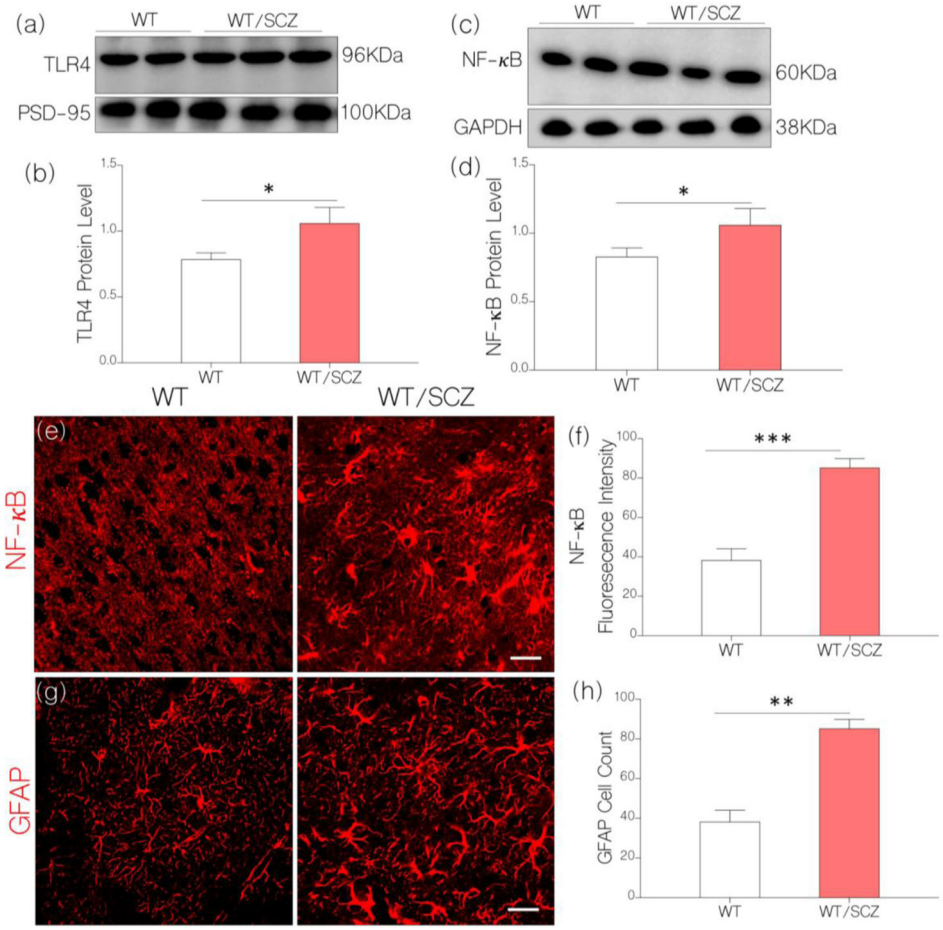

Figure 3.

a, Quantitative immunoblots show the expression of TLR4 in brain tissue lysate. The intensity of TLR4 was normalized by the corresponding PSD-95 and GAPDH expression.

b, Bar chart illustrating an increase in normalized neural TLR4 expression for WT/SCZ mice ($p<0.05$) when compared with the control (WT).

c, Immunoblot show normalized expression of NF-κB in the brain tissue lysate of control (WT) and WT/SCZ mice.

d, Bar chart demonstrating upregulated (normalized) NF-κB expression for WT/SCZ mice when compared with the control (WT; $p<0.05$).

e, Confocal images (scale bar=20μm) illustrating an increased neural NF-κB expression (normalized fluorescence intensity) for WT/SCZ mice when compared with the control (WT; $p<0.001$)

f, Statistical comparison of NF-κB fluorescence intensity for WT/Control and WT/SCZ groups.

g, GFAP positive cell count increased per unit area (astrocyte/μm^2) in the cortex of WT/SCZ mice when compared with the control ($p<0.01$; scale bar=20μm).

h, Bar charts illustrating the comparative distribution of GFAP positive cells in the brain of control (WT) and WT/SCZ mice.

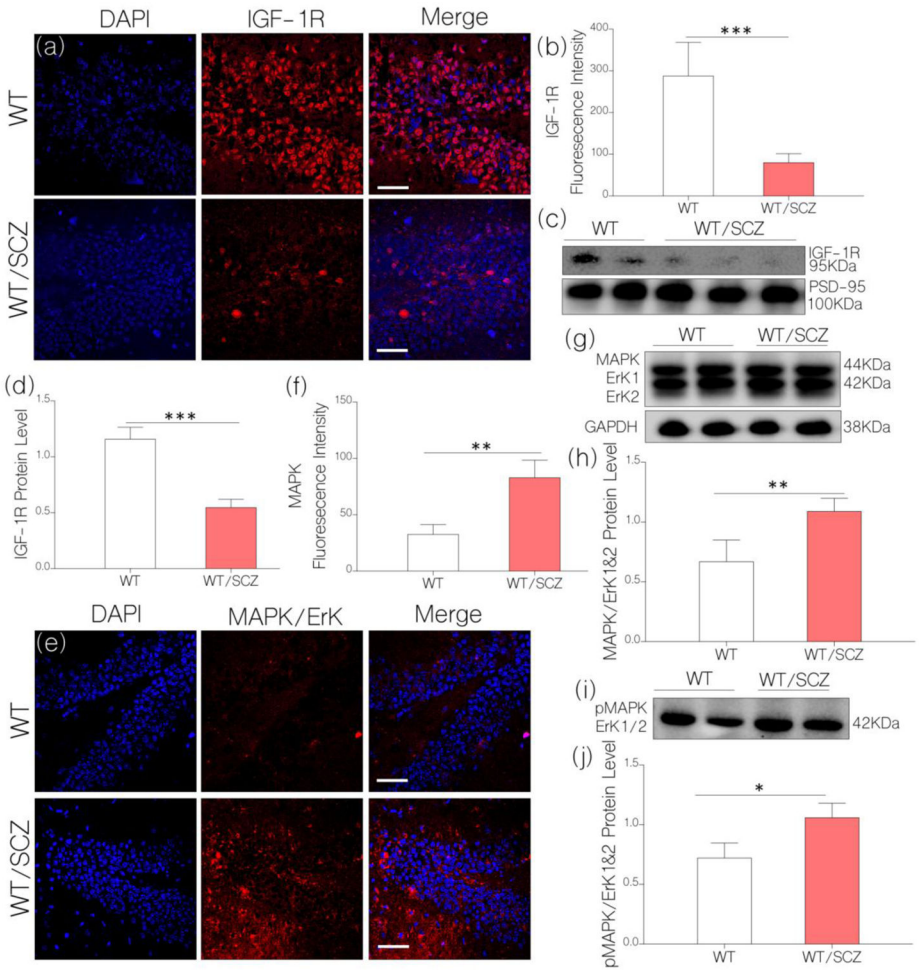

Figure 4.

a, Illustrative confocal images show a decrease in hippocampal IGF-1R expression for WT/SCZ mice ($p<0.001$) when compared with the control (scale bar=20μm).

b, Bar chart illustrating normalized fluorescence intensity for IGF-1R expression in WT (control) and WT/SCZ hippocampus.

c, Quantitative immunoblots show a significant decrease in neural IGF-1R expression for WT/SCZ mice when compared with the control (WT; $p<0.001$).

d, Bar chart demonstrating normalized IGF-1R protein level for WT (control) and WT/SCZ brain lysate.

e, Representative confocal images (scale bar=20μm) show an increased MAPK/ErK1/ErK2 expression for WT/SCZ hippocampus when compared with the control (WT; $p<0.01$).

f, Bar chart illustrating a comparative MAPK/ErK expression for WT and WT/SCZ hippocampus.

g, Quantitative immunoblots show MAPK/ErK1/ErK2 expression in hippocampal lysate of WT and WT/SCZ mice. MAPK/ErK ($p<0.01$) increased in the hippocampal lysate of WT/SCZ mice when compared with the control (WT).

h, Bar charts depicting statistical change in normalized MAPK/ErK expression in hippocampal lysate of WT (control) and WT/SCZ mice.

i, Western blot demonstrating an increased pMAPK/ErK1/ErK2 expression in hippocampal lysate of WT/SCZ mice when compared with the control ($p<0.05$).
j, Bar charts depicting statistical change in normalized pMAPK/ErK expression in hippocampal lysate of WT (control) and WT/SCZ mice.

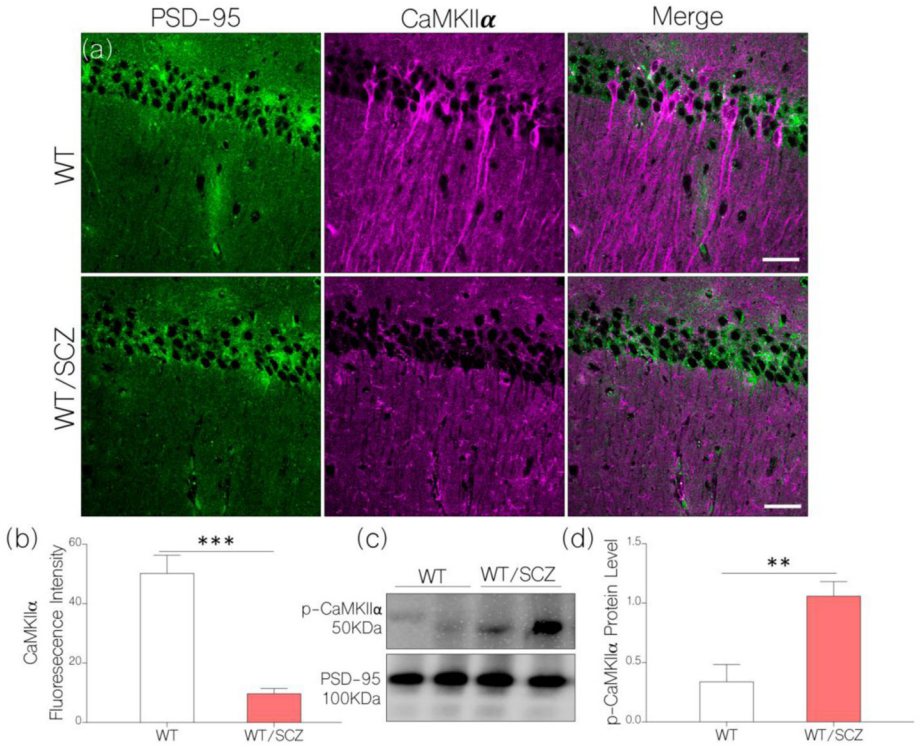

Figure 5.

a, Representative confocal images (scale bar=20μm) show a significant decrease in hippocampal CaMKIIα after NMDAR hypofunction was induced (WT/SCZ) in mice ($p<0.001$): versus the control (WT).

b, Bar chart comparing the expression of hippocampal CaMKIIα for control (WT) and behaviorally deficient NMDAR hypofunction mice (WT/SCZ).

c, Quantitative immunoblot and ***d***, bar chart shows increased phosphorylation of CaMKIIα in hippocampal lysate of WT/SCZ mice when compared with the control ($p<0.01$).

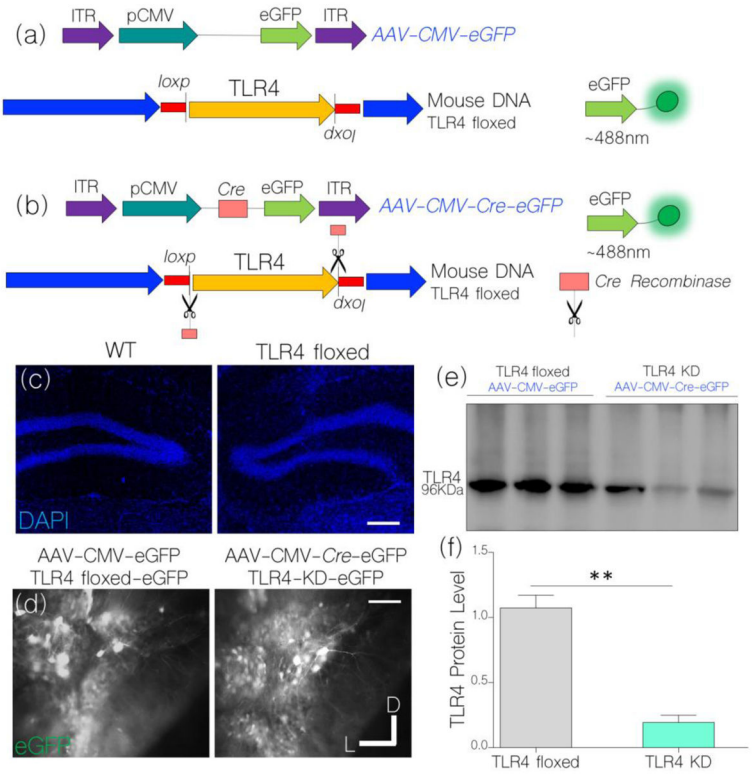

Figure 6.

a, Schematic illustration of control AAV expression (AAV-CMV-eGFP) in the TLR4 floxed mice.

b, *Cre-mediated* TLR4 knockdown (KD) following AAV-CMV-Cre-eGFP expression in the hippocampus of TLR4 floxed mice.

c, Fluorescence nuclear stain (DAPI) show a similar hippocampal (cellular) morphology for WT and TLR4 floxed mice (scale bar=40μm).

d, Fluorescence expression of eGFP reporter conveyed by AAV-CMV-eGFP and AAV-CMV-Cre-eGFP in the DG/CA1 field of TLR4 floxed mice 3 weeks *post-injection* (scale bar=30μm).

e, Western blots show a significant decrease in normalized TLR4 expression in hippocampal lysate of untreated TLR4 knockdown mice (AAV-CMV-Cre-eGFP), when compared with the untreated TLR4 floxed mice (AAV-CMV-eGFP) ($p<0.001$).

f, Bar chart illustrating statistical comparison (T-test) for normalized TLR4 expression in untreated TLR4 floxed and knockdown mice.

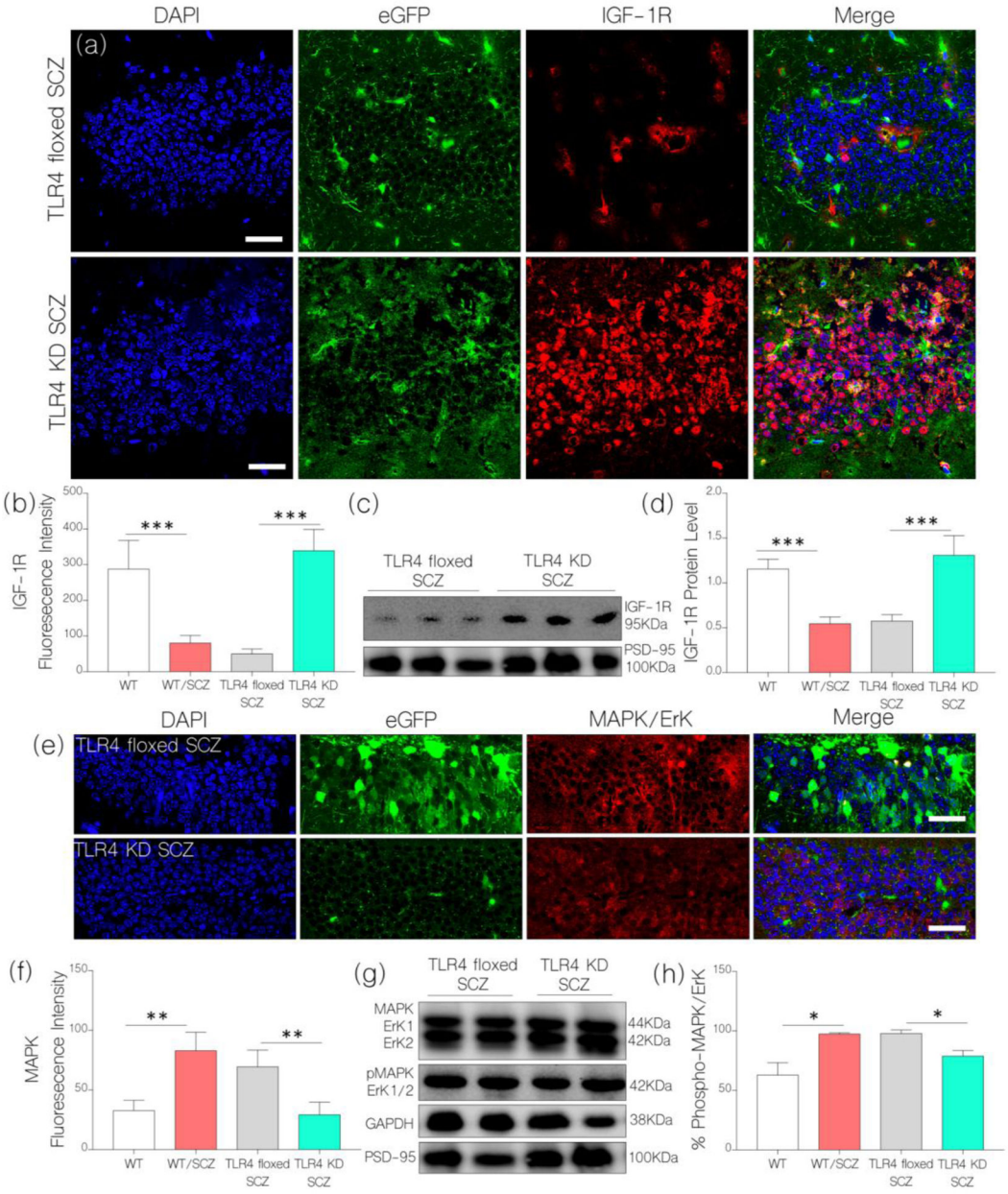

Figure 7.

a, Illustrative confocal images (scale bar=20μm) show a sustained hippocampal IGF-1R expression for TLR4 knockdown mice (TLR4 KD) after NMDAR hypofunction was induced (TLR4 KD SCZ). As such, TLR4 KD SCZ mice recorded an upregulated hippocampal IGF-1R expression when compared with TLR4 floxed SCZ and WT/SCZ mice ($p<0.001$). Additionally, there was no significant difference when TLR4 KD SCZ was compared with WT (control).

b, Bar chart depicting a comparative hippocampal IGF-1R expression (fluorescence intensity) for WT, WT/SCZ, TLR4 floxed SCZ, and TLR4 KD SCZ mice (One-Way ANOVA).

c, Immunoblots show a sustained neural IGF-1R expression in hippocampal lysate of TLR4 KD SCZ mice when compared with the TLR4 floxed SCZ mice ($p<0.001$). TLR4 floxed SCZ mice show a reduction in IGF-1R ($p<0.001$) when compared with the control (WT).
d, Bar chart showing normalized IGF-1R protein level in hippocampal brain lysate of WT, WT/SCZ, TLR4 floxed SCZ, and TLR4 KD SCZ mice.
e, Representative confocal images show increased MAPK/ErK1/ErK2 expression for TLR4 floxed SCZ ($p<0.01$) but not TLR4 KD SCZ mice after NMDAR hypofunction was induced; versus the control (WT).
f, Bar chart illustration of hippocampal MAPK/ErK1/ErK2 expression for WT, WT/SCZ, TLR4 floxed SCZ, and TLR4 KD SCZ mice.
g, Immunoblots show a change in MAPK/ErK1/ErK2 and pMAPK/ErK expression in hippocampal lysate of TLR4 floxed SCZ and TLR4 KD SCZ mice. There was a significant decrease in percentage phosphorylated MAPK/ErK (pMAPK/ErK) for TLR4 KD SCZ mice when compared with TLR4 floxed SCZ and WT/SCZ mice ($p<0.05$).
h, Bar chart depicts comparative (One-Way ANOVA) percentage phosphorylation of MAPK/ErK in hippocampal lysate of WT, WT/SCZ, TLR4 floxed SCZ, and TLR4 KD SCZ mice.

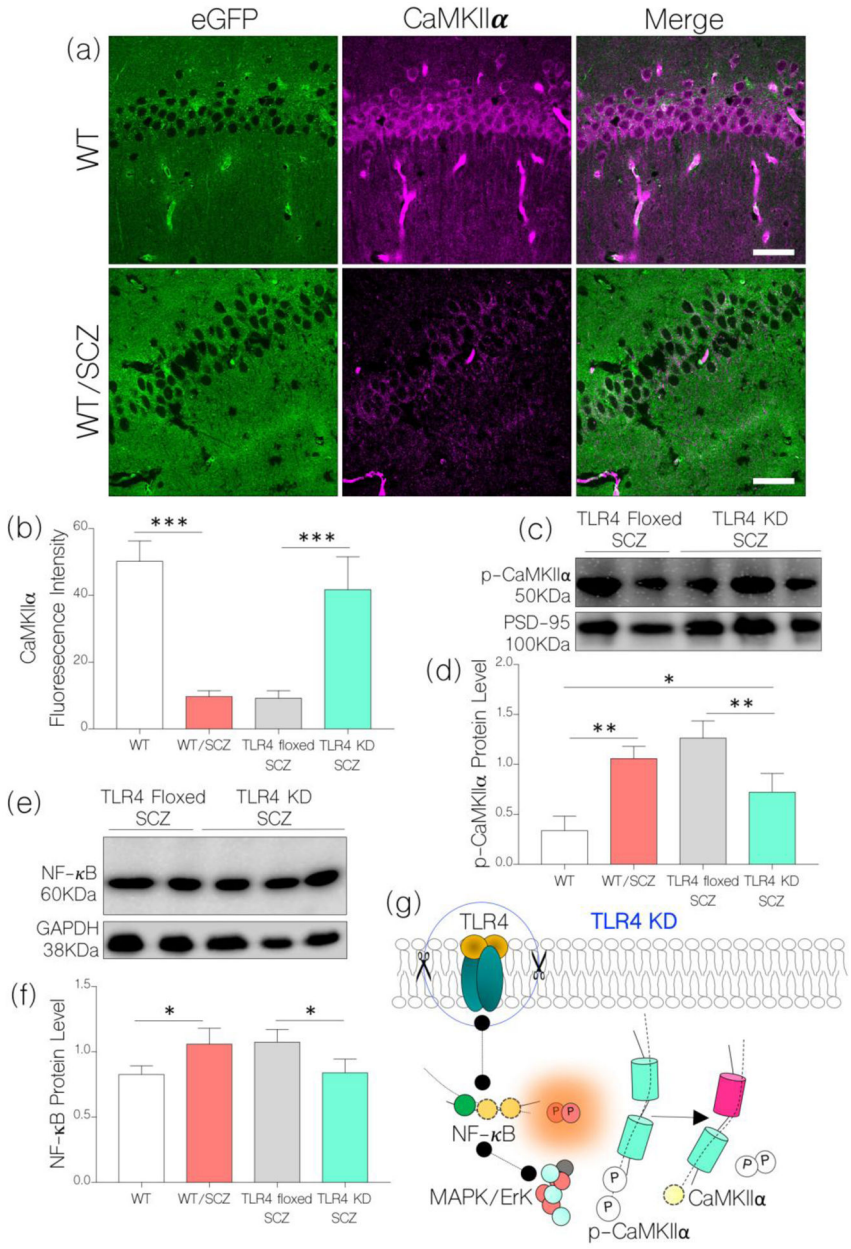

Figure 8.

a, Representative confocal images show sustained expression of CaMKIIα in the hippocampus of TLR4 KD SCZ mice after an induced NMDAR hypofunction. When compared with the WT (control), no significant change in CaMKIIα expression was recorded. Like WT/SCZ, neural CaMKIIα expression reduced significantly in TLR4 floxed SCZ mice when compared with the control ($p<0.001$).

b, Bar chart illustrating comparative (normalized) expression of CaMKIIα in the hippocampus of WT, WT/SCZ, TLR4 floxed SCZ, and TLR4 KD SCZ mice (One-Way ANOVA).

c, Western blot and ***d,*** bar chart showing a change in phosphorylated CaMKIIα (p-CaMKIIα) in hippocampal lysate of TLR4 KD SCZ and TLR4 floxed SCZ mice.
e, Immunoblot and ***f,*** bar chart shows a reduced NF-κB expression in hippocampal lysate of TLR4 KD SCZ when compared with TLR4 floxed SCZ mice ($p<0.05$). No significant change in NF-κB was recorded for the TLR4 KD SCZ group when compared with the control (WT).
g, Schematic illustration of a possible mechanism through which TLR4 knockdown might have attenuated hippocampal CaMKIIα loss and restored NMDAR function in schizophrenia.

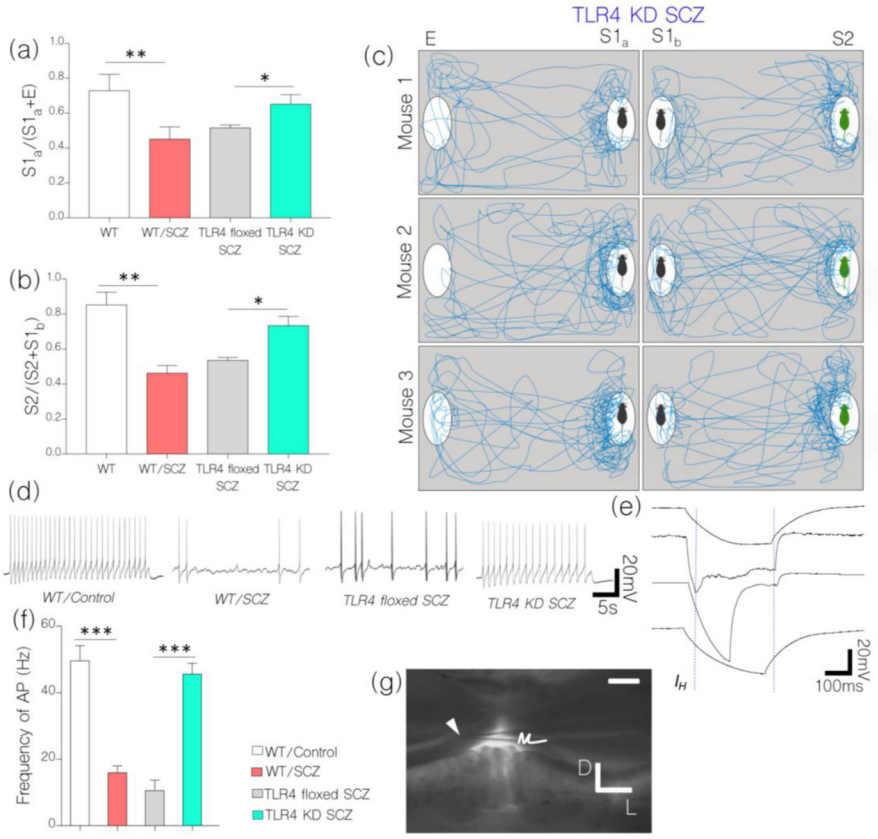

Figure 9.

a, Bar chart illustrating sociability test outcome for WT, WT/SCZ, TLR4 floxed SCZ, and TLR4 KD SCZ mice (One-Way ANOVA). TLR4 KD SCZ mice show an improvement in sociability behavior by expressing preference for $S1_a$ over E ($p<0.05$) versus TLR4 floxed SCZ and WT/SCZ mice. Conversely, TLR4 floxed SCZ mice recorded a decline in sociability behavior like the WT/SCZ.

b, Bar chart illustrating social novelty test outcome for WT, WT/SCZ, TLR4 floxed SCZ, and TLR4 KD SCZ mice (One-Way ANOVA). TLR4 KD SCZ mice showed an improvement in social novelty with preference for $S2$ over $S1_b$. TLR4 floxed SCZ mice recorded a decline in social novelty like the WT/SCZ group ($p<0.05$).

c, Drawing of traced movement path for TLR4 KD SCZ mice in sociability and social novelty tests.

d, NMDAR hypofunction (WT/SCZ) caused a significant decrease in the frequency of evoked action potential (Hz) in hippocampal neurons when compared with the control ($n=7$; $p<0.001$). Similarly, TLR4 floxed SCZ neurons recorded a decrease in frequency action potential (mV) after NMDAR hypofunction was induced ($p<0.001$). Interestingly, TLR4 KD SCZ neurons recorded no significant change in evoked action potential when compared with the control (ns). Together, control (WT) and TLR4 KD SCZ mice were characterized by tonic firing while WT/SCZ and TLR4 floxed SCZ neurons exhibited an irregular gap firing pattern.

e, Hippocampal neurons of WT/SCZ and TLR4 floxed SCZ mice elicited abnormally prolonged K^+-linked after-hyperpolarization phase (AHP) (n=9); versus the control (WT). No abnormal AHP was recorded for TLR4 KD SCZ hippocampal neurons.

f, Bar chart show a change in frequency of action potential for hippocampal neurons of WT/SCZ, TLR4 floxed SCZ, and TLR4 KD SCZ mice.

g, Location of the patch pipette electrode (arrow head) in the hippocampus (scale bar=100μm) during acute slice electrophysiological (patch clamping) recording.

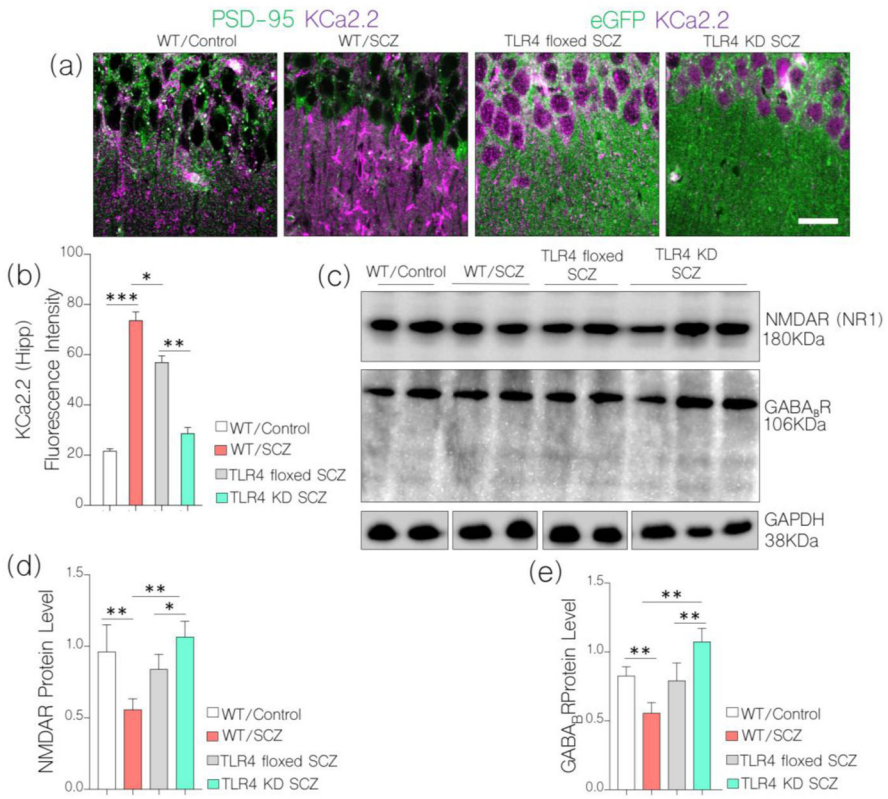

Figure 10.

a, Representative confocal images and ***b,*** bar chart demonstrating increased KCa2.2 expression at post-synaptic densities for WT/SCZ ($p<0.001$) and TLR4 floxed SCZ ($p<0.01$) hippocampus (scale bar=20μm) when compared with WT (control) and TLR4 KD SCZ. ***c,*** Western blots show the expression of NMDAR and $GABA_BR$ in the hippocampus of WT, WT/SCZ, TLR4 floxed SCZ, and TLR4 KD SCZ mice. TLR4 knockdown prevented loss of NMDAR ($p<0.05$) and $GABA_BR$ ($p<0.01$) after NMDAR hypofunction was induced. ***d–e,*** Bar chart demonstrating normalized level of NMDAR and $GABA_BR$ in hippocampal WT, WT/SCZ, TLR4 floxed SCZ, and TLR4 KD SCZ.

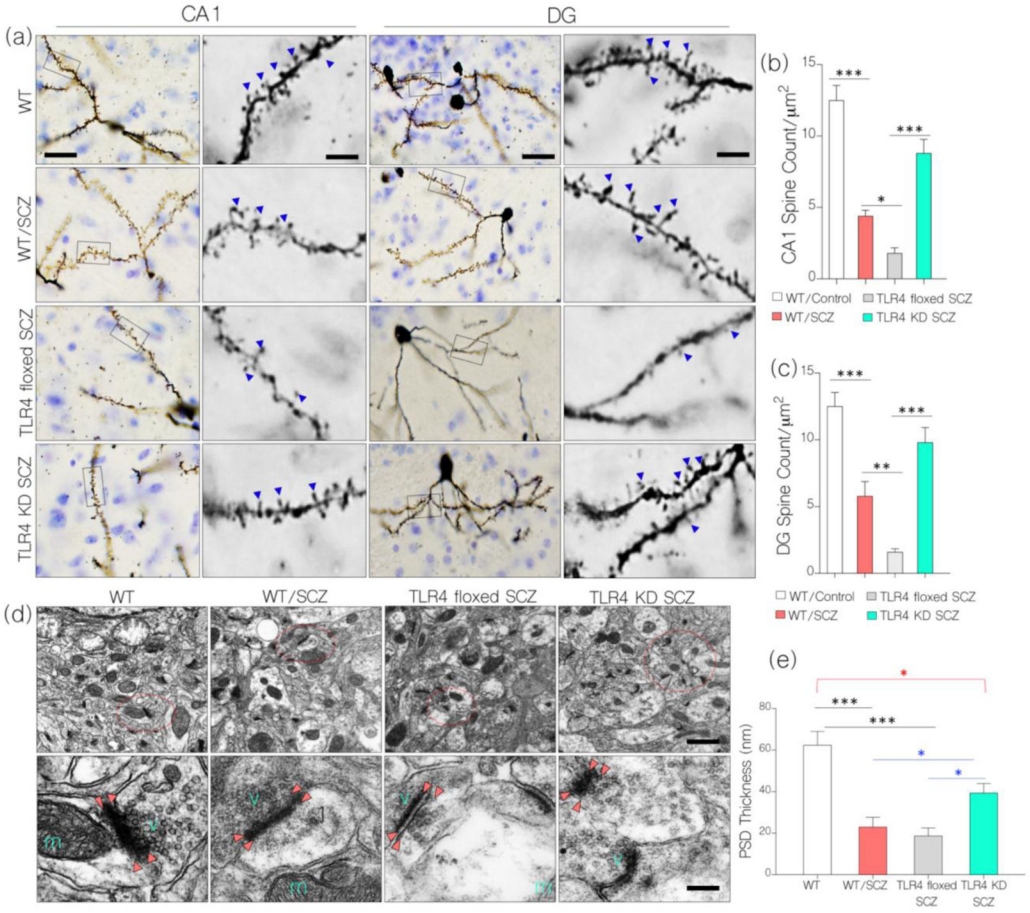

Figure 11.

a, Photomicrographs show Golgi-Cox stained hippocampal neurons. At higher magnification, the distribution of dendritic spines was quantified serologically in the hippocampus. WT/SCZ and TLR4 floxed SCZ mice showed a significant decrease in CA1 ($p<0.001$) and DG ($p<0.001$) dendritic spine count when compared with the control. In subsequent analysis, TLR4 floxed SCZ mice showed a significant decrease compared with the WT/SCZ group (CA1: $p<0.05$, DG: $p<0.01$). In TLR4 KD SCZ loss of dendritic spines was significantly attenuated when compared with the other experimental SCZ groups ($p<0.05$), but was less versus the control ($p<0.05$; scale bar=20μm, 5μm).

b–c, Bar chart depicting statistical change in DG/CA1 dendritic spine count for the experimental SCZ groups and control.

d, Transmission Electron Microscopic images (scale bar=500nm, 100nm) show change in synaptic morphology for the experimental SCZ groups when compared with the control. WT/SCZ and TLR4 floxed SCZ mice show decreased post-synaptic density thickness (nm; bright red arrow heads) when compared with the control (WT; $p<0.001$). Additionally, WT/SCZ and TLR4 floxed SCZ recorded a significant increase in synaptic cleft diameter when compared with the control ($p<0.001$). These changes were attenuated in TLR4 KD SCZ hippocampus.

e, Bar chart show statistical change in post-synaptic density thickness for the experimental SCZ groups when compared with the control.